University of Crete

Department of Physics

Master Thesis

Submitted in partial fulfilment
of the requirements for the degree of
Master of Science in Advanced Physics

Probing Dark Energy with Cosmic Structures

Author:
Dimitrios Tanoglidis

Supervisor:
Prof. Vasiliki Pavlidou
Co-Supervisor:
Prof. Theodore Tomaras

Heraklion
June 2016

E.S. (R)

"But now I have come to believe that the whole world is an enigma, a harmless enigma that is made terrible by our own mad attempt to interpret it as though it had an underlying truth."

Umberto Eco

Acknowledgements

It is a pleasure for me to thank my supervisors, Profs. Vasiliki Pavlidou and Theodore Tomaras, for the support during my studies and during the work for this thesis. Their guidance helped me not only to try to become a better physicist, but also to overcome my fears and dare to target for high goals. I will do my best to prove that I am worthy of the great opportunity they gave me.
I would like like also to thank all my colleagues and friends these years who made my life better even during difficult times. Last but not least, all the people who supported me, both financially and morally, during a very tough period.
Research implemented under the ARISTEIA II Action of the Operational Program Education and Lifelong Learning and is co-funded by the European Social Fund (ESF) and Greek National Resources. This work was also supported by by the European Commission Seventh Framework Programme through grants PCIG10-GA-2011-304001 JetPop and PIRSES-GA-2012-31578 EuroCal.

Abstract

The presence of a dark energy component in the Universe has a profound effect on the evolution of cosmic structure: acting as anti-gravity, halts structure growth. In the present work we use this effect to probe dark energy. We propose the *turnaround radius* of cosmic structures as the optimum observable quantity where the effect of dark energy is imprinted. We consider the standard ΛCDM cosmology (where the dark energy behaves as a cosmological constant) and cosmologies with a dark energy with a more general equation of state parameter, w. We demonstrate that, in the context of the ΛCDM model, it is in principle possible to measure the value of the cosmological constant by tracing, across cosmic time, the evolution of the turnaround radius of cosmic structures. The novelty of the presented method is that it is local, in the sense that it uses the effect of the cosmological constant on the relatively short scales of cosmic structures and not on the dynamics of the Universe at its largest scales. In this way, it can provide an important consistency check for the standard cosmological model and can give signs of new physics, beyond ΛCDM. We extend the method for a more general equation of state parameter, w, and we show that the evolution of turnaround radius depends clearly on it, and thus can be used to constrain it.

Contents

Chapter 1

A Brief Review of Cosmology

This chapter serves as a brief review of Cosmology. We will present the equations describing the evolution of a homogeneous and isotropic Universe, which depends on its content. The equations and the notation we will develop here, although presented for the case of the Universe at its largest scales (where it is homogeneous and isotropic) will be used later to describe the evolution of structure in it. Detailed derivation of the formulae will not be presented, since this is beyond the scope of this thesis. The interested reader can find the derivations in the books mentioned in the bibliography.

1.1 Dynamics of the Expanding Universe

The Universe at its largest scales ($\sim >$ 100Mpc, where 1 pc $\cong 3.086 \times 10^{16} m$) is homogeneous and isotropic. We also have evidence that it is expanding: Hubble first discovered in 1920's that distant galaxies move away from us with a speed which is proportional to their distance (Hubble's law). This observation, combined with the *Cosmological Principle* which states that we do not have any privileged position in the Universe, which looks the same at each point, leads to the picture of an expanding Universe.

We can describe this effect by introducing the concept of the **scale factor**, a, and by convention set that $a_0 = 1$ (i.e. its present value. Everywhere in this thesis a subscript of "0" denotes the present epoch). The scale factor is characterising the relative size of a (large - as for the conditions of homogeneity and isotropy to be valid) spatial section normalized to the present value and depends on time:

$$a(t) \equiv \frac{R(t)}{R_0}. \tag{1.1.1}$$

Our task here is to derive equations that describe the evolution of the scale factor with time. This evolution depends on the content of the Universe.

The scale factor is also related to another useful concept, the **redshift**, z. Observationally, the redshift is defined as the the change of the wavelength of an emitted photon, due to its radial motion relative to us:

$$z \equiv \frac{\lambda_{\rm obs} - \lambda_{\rm em}}{\lambda_{\rm em}}, \tag{1.1.2}$$

where $\lambda_{\rm obs}$ is the observed wavelength and $\lambda_{\rm em}$ the emitted wavelength of the photon. For a source that recedes with (radial) velocity υ, it is related with it as:

$$1+z=\sqrt{\frac{1+\upsilon/c}{1-\upsilon/c}}, \tag{1.1.3}$$

where c is the speed of light. For small values of υ we have $z\cong\upsilon/c$. Now, for a photon emitted at a time t and observed today, the following relation between the scale factor $a(t)$ and the redshift holds:

$$a(t)=\frac{1}{1+z}\qquad\Leftrightarrow\qquad z=\frac{1}{a(t)}-1. \tag{1.1.4}$$

Now, we can sketch the derivation of the equations that determine the evolution of the scale factor. To study the Universe we need the theory of General Relativity (GR). According to it, the metric of the spacetime is related to the energy content of the Universe through **Einstein's equations**:

$$\boxed{R_{\mu\nu}-\frac{1}{2}Rg_{\mu\nu}=8\pi GT_{\mu\nu},} \tag{1.1.5}$$

where we have set $c=1$ and G being Newton's gravitational constant, $G\cong 6.6738(8)\times10^{-11}\,\mathrm{m^3\,kg^{-1}\,s^{-2}}$. $R_{\mu\nu}$ and R are known as the Ricci tensor and Ricci scalar, respectively, and are contractions of the Riemann tensor, which in turn is a complicated combination of derivatives of the **metric**, $g_{\mu\nu}$. For details, the reader is referred to the bibliography. $T_{\mu\nu}$ is known as the **energy-momentum tensor** describes the density and the flux of energy and momentum in spacetime of the constituents of the Universe.

As we have have already noted, at its largest scales the Universe is homogeneous and isotropic. This helps us to write down an ansatz for the metric of spacetime. The metric is a "ruler" that allows to measure distances in spacetime. For spatial part being homogeneous and isotropic, the metric takes the **Friedmann-Robertson-Walker (FRW)** form:

$$ds^2=g_{\mu\nu}dx^\mu dx^\nu=-dt^2+a^2(t)R_0^2\left[\frac{dr^2}{1-kr^2}+r^2\left(d\theta^2+\sin^2\theta d\phi^2\right)\right]. \tag{1.1.6}$$

The parameter k is known as the **curvature parameter** and can take the values $+1,0,-1$. These correspond to the three possibilities of a positively curved (closed), flat and negatively curved (open) Universe. These are 3D analogues to a surface of a sphere, a flat surface and the surface of a hyperboloid (saddle). The coordinates of the spatial part of the metric, as written here, are known as the **comoving coordinates**. The metric $g_{\mu\nu}$ is:

$$g_{\mu\nu}=\mathrm{diag}\left(-1,\frac{a^2(t)R_0^2}{1-kr^2},a^2(t)R_0^2r^2,a^2(t)R_0^2r^2\sin^2\theta\right). \tag{1.1.7}$$

From this and its inverse, $g^{\mu\nu}$, can be computed the left hand side of eq. (1.1.5).

In order to proceed, we need to specify the form of the energy-momentum tensor. The content of the Universe can be modelled as a perfect fluid of density $\rho(t)$ and $p(t)$. The energy-momentum tensor of such a fluid is

$$T_{\mu\nu}=(\rho+p)\,U_\mu U_\nu+pg_{\mu\nu}, \tag{1.1.8}$$

with U^μ being the four velocity of the fluid. For an isotropic fluid its four velocity is $U_\mu = (1, 0, 0, 0)$. The energy-momentum tensor is:

$$T_{\mu\nu} = \mathrm{diag}\left(\rho, pg_{11}, pg_{22}, pg_{33}\right) \qquad \text{or} \qquad T^\mu{}_\nu = \mathrm{diag}(-\rho, p, p, p). \tag{1.1.9}$$

With the ansatz of the FRW metric and the energy-momentum tensor (1.1.9), the Einstein equations reduce to the **Friedmann Equations**:

$$\boxed{\left(\frac{\dot{a}}{a}\right)^2 = \frac{8\pi G}{3}\rho - \frac{k}{a^2 R_0^2}} \tag{1.1.10}$$

and

$$\boxed{\frac{\ddot{a}}{a} = -\frac{4\pi G}{3}\left(\rho + 3p\right).} \tag{1.1.11}$$

The overdots denote differentiation with respect to t. The second of these is also known as the **acceleration equation**. Note that in order for the Universe to be accelerating, we must have $p/\rho < -1/3$. Another, but not independent, equation can be derived from the energy conservation (in its relativistic form):

$$\nabla_\mu T^\mu{}_0 = 0 \qquad \Rightarrow \qquad \dot{\rho} + 3\frac{\dot{a}}{a}\left(\rho + p\right) = 0. \tag{1.1.12}$$

This is known as the **continuity equation**.

Now we have two independent equations for three unknowns, namely $a(t), \rho(t), p(t)$. To close the system of equations, we need one more. This is the **equation of state**, which relates the pressure and the density of the fluid. Perfect fluids, relevant to cosmology obey the simple equation of state:

$$p(t) = w\,\rho(t), \tag{1.1.13}$$

where the parameter w is known as the **equation of state parameter**. Different components of the the Universe have different values of w:

$$w = \begin{cases} 0, & \text{matter} \\ +\frac{1}{3}, & \text{relativistic matter (radiation)} \\ \text{-1}, & \text{cosmological constant} \\ < -\frac{1}{3}, & \text{dark energy (general form)} \end{cases}. \tag{1.1.14}$$

Assuming constant equation of state parameter, we have (from the continuity equation, (1.1.12)) the evolution of the density of a component of the Universe (assuming no couplings between components):

$$\rho(t) = \frac{\rho_0}{a(t)^{3(1+w)}}, \tag{1.1.15}$$

where ρ_0 is the density at present time. Also, for a flat ($k = 0$) Universe, dominated by just one component with constant equation of state, the evolution of the scale factor is given by:

$$a(t) = \left(\frac{t}{t_0}\right)^{\frac{2}{3(1+w)}}, \tag{1.1.16}$$

where t_0 is the current age of the Universe. If there are more than one dominant components, one has to solve Friedmann equation numerically.

1.2 Cosmological Parameters

The expansion rate of the Universe is called the **Hubble parameter** and is defined as:

$$H \equiv \frac{\dot{a}}{a}. \tag{1.2.1}$$

The Hubble parameter at the present epoch is known as the **Hubble constant**, H_0 and is usually written in terms of the dimensionless parameter h as:

$$H_0 = 100h \text{ km s}^{-1} \text{ Mpc}^{-1}. \tag{1.2.2}$$

with the parameter h including all the uncertainty. The present value is $h = 0.721$. Note that with this definition of the Hubble parameter, the left hand side of the Friedmann equation, eq. (1.1.10) can be written as H^2.

From the Friedmann equation, eq. (1.1.10) we can see that there is a critical value of the energy density such that the Universe has flat spatial geometry ($k = 0$). This is known as the **critical density** and is:

$$\rho_{\text{crit}} \equiv \frac{3H^2}{8\pi G}. \tag{1.2.3}$$

The current critical density is:

$$\rho_{\text{crit},0} = 1.88 \times 10^{-26} h^2 \quad \text{kg m}^{-3}. \tag{1.2.4}$$

Usually, the total energy density is measured in terms of the critical density. For this reason, we introduce the dimensionless **density parameter**:

$$\boxed{\Omega \equiv \frac{\rho}{\rho_{\text{crit}}}} \tag{1.2.5}$$

This parametrization connects the value of Ω with the spatial geometry:

$$k = \text{sgn}(\Omega - 1). \tag{1.2.6}$$

It also allows to write Friedmann equation (1.1.10), in a useful way:

$$H^2(\Omega - 1) = \frac{k}{R_0}. \tag{1.2.7}$$

Of course, beyond the total energy density parameter, we can also define the density parameter of each component of the Universe as:

$$\Omega_i = \frac{\rho_i}{\rho_{\text{crit}}}, \tag{1.2.8}$$

with i denoting matter, radiation, dark energy, curvature.

1.3 Distances

Measuring distances in the Universe is important (indeed, to measure its expansion rate we need to measure distances, of distant supernovae, for example). But it

is also difficult and tricky, since the Universe is expanding. Here we will present some frequently used distance measures.

Let start by defining some "time distances". The age of the Universe is related to the expansion history by:

$$t = \int_0^t dt' = \int_0^a \frac{da'}{a' H(a')}. \tag{1.3.1}$$

Another important quantity is the (comoving) distance light could have travelled since $t = 0$, known as the **comoving horizon** (remember we have set $c = 1$):

$$\eta \equiv \int_0^t \frac{dt'}{a(t')}. \tag{1.3.2}$$

Regions separated by distance greater than η are not casually connected. η can be also considered as a time variable, called **conformal time**.

An important quantity is the **comoving distance**, χ, to a distant object at scale factor a (or redshift z):

$$\chi(a) = \int_{t(a)}^{t_0} \frac{dt'}{a(t')} = \int_a^1 \frac{da'}{a'^2 H(a')} \left(= \int_0^z \frac{dz'}{H(z')} \equiv \chi(z) \right). \tag{1.3.3}$$

As we will just see, the comoving distance is related to the other distance measures used in cosmology.

A frequently used method to determine distances in astronomy and cosmology is through measuring the angular size, θ, on the sky of an object of known physical size, ℓ. For small angles, the **angular diameter distance** is defined as:

$$d_A \equiv \frac{\ell}{\theta}. \tag{1.3.4}$$

For a flat Universe, the angular diameter distance is connected to the comoving distance χ as:

$$d_A = a \cdot \chi(a) = \frac{\chi(z)}{1+z}. \tag{1.3.5}$$

Another way to measure distances is through measuring the observed flux, F, from a source of known intrinsic luminosity, L. The flux is related to the distance of the source, d, as:

$$F = \frac{L}{4\pi d^2}. \tag{1.3.6}$$

We thus define the **luminosity distance**:

$$d_L \equiv \sqrt{\frac{L}{4\pi F}}. \tag{1.3.7}$$

In an expanding Universe, it can be shown that the luminosity distance is related to the comoving distance as:

$$d_L = \frac{\chi(a)}{a} = \chi(z) \cdot (1+z). \tag{1.3.8}$$

From eqs. (1.3.5) and (1.3.8), it turns out that the following relation must hold:

$$d_L = (1+z)^2 d_A \tag{1.3.9}$$

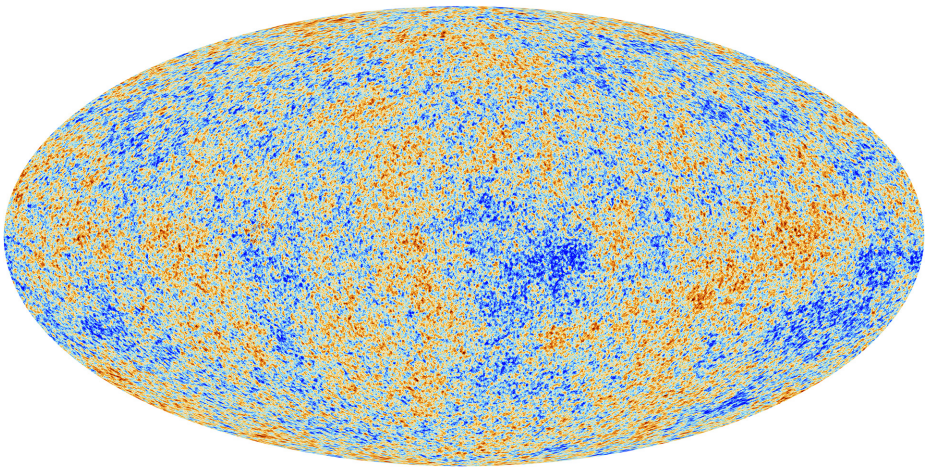

Figure 1.1: Cosmic Microwave Background temperature anisotropies, as measured from the Planck satellite.

1.4 The Cosmic Microwave Background

One of the most powerful probes of cosmology is the Cosmic Microwave Background (CMB), the afterglow of the Big Bang. When the Universe was very young and hot, photons and matter had huge energies. They scattered at huge rates and so they remained tightly coupled and the Universe was opaque. As the Universe expanded , it cooled down. At some moment its temperature dropped below the binding energies of typical atoms. Then electrons started getting bound to nuclei forming neural atoms, in a process known as **recombination** (although a better name would be just "combination", since it was the first time atoms formed). Because of recombination, photons could no longer scatter of free electrons and then radiation decoupled from matter; thus this process is called **decoupling**. These processes happened at a redshift of $z \cong 1100$, or about 380.000 years after the Big Bang.

The surface where these process took place is called the last scattering surface. Photons started free-streaming from that moment; i.e. they were moving freely through the Universe. The photons which form the CMB had their last interaction with matter at the last scattering surface. By measuring the properties of these photons today (temperature, anisotropy, polarization) we can obtain information about the last scattering surface and the Early Universe.

CMB is the most perfect blackbody. As the Universe expands after the epoch of decoupling , it retains its blackbody shape, with decreasing temperature. Today this temperature is $T_0 \cong 2.7266K$ and it is almost isotropic. There are small intrinsic temperature anisotropies of the order of $10^{-5}K$, which carry important information for the first moments of the Universe, as well as they provide the seeds for the formation and evolution of cosmic structure. Figure 1.1 shows temperature anisotropies (exaggerated, compared to the real temperature anisotropies) as measured from the Planck satellite.

As any function on the surface of the sphere, we can decompose the temperature pattern in spherical coordinates $\{\theta, \phi\}$:

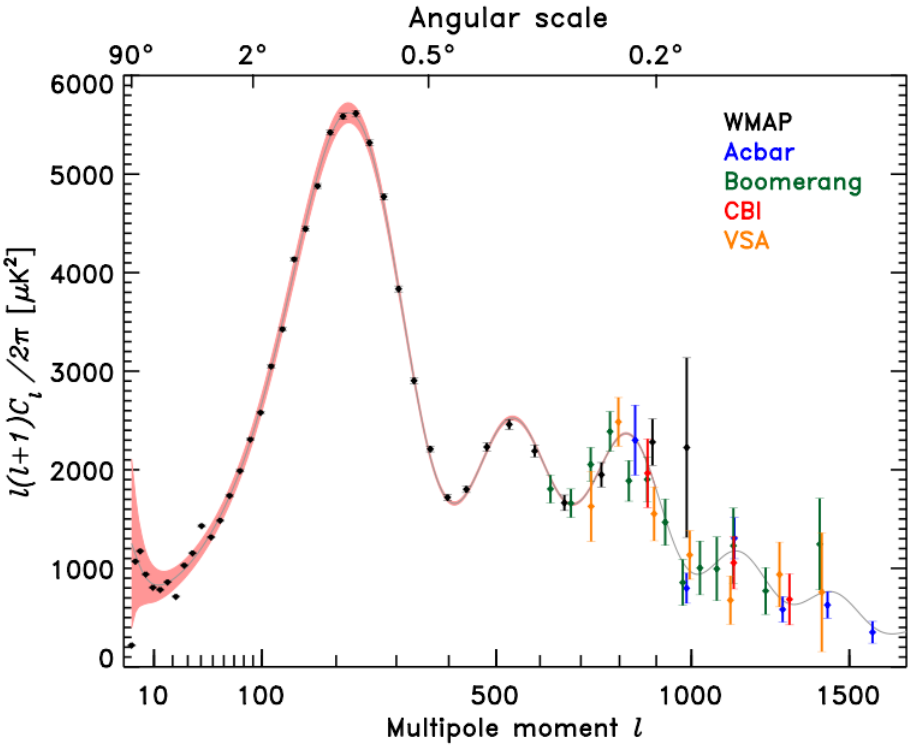

Figure 1.2: The temperature power spectrum of the CMB

$$\frac{\Delta T(\theta,\phi)}{T_0} = \sum_{\ell=0}^{\infty} \sum_{m=-\ell}^{\ell} a_{\ell m} Y_{\ell m}(\theta,\phi), \tag{1.4.1}$$

where $\Delta T(\theta,\phi) = T(\theta,\phi) - T_0$ is the difference from the mean temperature and $Y_{\ell m}(\theta,\phi)$ are the spherical harmonics. Coefficients $a_{\ell m}$ are connected to the multipole moments C_ℓ:

$$C_\ell \equiv \left\langle |a_{\ell m}|^2 \right\rangle = \frac{1}{2\ell+1} \sum_m |a_{\ell m}|^2 . \tag{1.4.2}$$

The $\ell = 0$ is the monopole, the average temperature. The $\ell = 1$ is the dipole, the Doppler effect, due to the motion of the Earth relative to the CMB rest frame. The intrinsic anisotropy corresponds to $\ell \geq 2$. A given multipole of order ℓ corresponds to angular separation on the sky:

$$\theta \cong \frac{180^\circ}{\ell}. \tag{1.4.3}$$

Plotting C_ℓ (or, more frequently the combination $\ell\,(\ell+1)$) versus ℓ we get the **power spectrum**, which gives the contribution of each multipole (and thus of each angular separation in the sky) to the variation of temperature in the sky. In other words, if a multipole dominates, it means that temperature anisotropies are more prominent in angular distances $\theta \cong 180^\circ/\ell$. In figure 1.2 the temperature power spectrum of the CMB is presented composed from a combination of measurements.

The most prominent feature of the power spectrum is a series of peaks, known as the **acoustic peaks**. These originate from the oscillations in the photon-electron plasma. Although the exact form of the spectrum has a complicated dependence on cosmology, the position in ℓ of the **first peak** can be easily predicted. It corresponds to the (angular) size of the sound horizon at decoupling. The angular size in which we finally observe this peak depends on the geometry (and thus of the density) of the Universe. In a Universe with positive curvature, photon paths will converge leading to a smaller observed angular size compared to that of a flat Universe (which would be exactly the predicted one). The opposite is true for a Universe with negative curvature. The connection between the observed value of $\ell_{\rm f.peak}$ and the total energy density of the Universe is:

$$\ell_{\rm f.peak} \cong 220\Omega^{-1/2}. \tag{1.4.4}$$

As it can be seen from the observed power spectrum, the position of the first peak is close to 220, thus in favour of a Universe very close to flat ($\Omega = 1$).

1.5 Summary: The Content of the Universe

In the following chapter we will see the observational evidence for the presence of a cosmological constant in the Universe, which accounts for the biggest part of the energy content of the Universe. For future convenience, let us present now the latest observational values for the cosmological parameters.

Density parameters (all refer to present values):

- Cosmological constant density parameter: $\Omega_\Lambda = 0.685^{+0.017}_{-0.016}$
- Matter density parameter: $\Omega_{\rm m} = 0.315^{+0.016}_{-0.017}$
- CMB radiation density of the Universe: $\Omega_\gamma = 5.46(19) \times 10^{-5}$

As you can see, observations point to a flat Universe ($\Omega = 1$). The constraints on the equation of state parameter of the dark energy are $w = -1.10^{+0.08}_{-0.07}$. Observations are thus still consistent with the hypothesis of a cosmological constant. The dimensionless Hubble parameter is:

$$h = 0.673(12). \tag{1.5.1}$$

So far we have talked about the homogeneous Universe. Indeed, at its largest scales ($>$ 100Mpc, where 1pc$\cong 3.086\times10^{16}m$) is to a very good approximation homogeneous and isotropic. But in smaller scales there are strong inhomogeneities: stars, galaxies, groups and clusters and superclusters of galaxies. Galaxies and especially the structures formed from galaxies, like the clusters, constitute the **Large Scale Structure (LSS)** of the Universe. A typical galaxy, such our own Galaxy, has a mass of $10^{11}\,M_\odot$, where $1M_\odot = 1.988 \times 10^{30}kg$, a solar mass. Clusters of galaxies can contain from 50-60 to thousands of galaxies. The local supercluster has a mass of $10^{14}M_\odot$. Two famous clusters are the Virgo cluster and the Coma cluster. In this thesis we will focus on how we can use cosmic structure to probe dark energy.

Chapter 2

Observational Probes of Dark Energy

There is now a large amount of observations suggesting that the Universe is accelerating. This acceleration is usually explained through postulating the existence of a dark energy component in the Universe, although proposals of modifications of standard gravity are also on the table. In the following chapter we will describe in brief these models. Here we review the main observational evidence for the existence of dark energy. Standard Candle and Standard Ruler methods are discussed. These methods are consider the effect of dark energy in the general dynamics of the Universe, i.e. effects on the largest scales. Later we will present a new, complementary, but also extremely useful way to probe dark energy on short scales, the scales of cosmic structures.

2.1 Early Indications for the Presence of Dark Energy

We will see in the following section that the first **direct** proof for an accelerating Universe and a cosmological constant came in 1998 with studies of distant supernovae. However, indirect indications existed before that date, pointing to the need for an accelerating Universe. Here we review them, focusing on the **cosmic age problem**, the fact that the Universe appeared to be younger than some of the oldest stars it contains.

A first such indication came from measurements of galaxy number densities. It was found that the number of galaxies in the distant Universe was larger (in the same size volume of space) than today. Since galaxy mergers are not so strong to reduce the number of galaxies, the only solution to the problem is that the calculation of number **densities** is not correct, because the volume of space was not correctly calculated. This could be the case if the Universe was accelerating and not decelerating as it was thought to be (and used in calculations). Although this was an appealing explanation, it was not widely accepted since it was thought that it was more probable that our knowledge of galaxy formation was not correct rather than our knowledge of gravity.

Another strong indication was (and it remains today) the **missing matter** problem. By measurements of masses of cluster (including dark matter), it was known that $\Omega_{\mathrm{m},0} \cong 0.3$. When it was thought that the Universe contains only matter, this was also the total energy density. Thus the Universe appeared to be open (sub-critical density). However, from inflation, a theory which explains the

homogeneity and isotropy, as well as the initial conditions for structure formation in the Universe, one expects the Universe to be very close to flat, $\Omega \sim 1$. Beyond this theoretical argument, from measurement of the first peak in the CMB power spectrum (see the discussion in section 1.4) there is strong evidence that the Universe is indeed flat (it was known before 1998, but now there are even better measurements of the position of the first peak). The discrepancy between the energy density required for the Universe to be flat and the measured matter density requires the introduction of another energy component which fills the gap. The simplest possible is the cosmological constant.

Let us consider now the cosmic age problem we mentioned before. The present day of a flat Universe which contains matter and cosmological constant ($\Omega_{\mathrm{m},0} + \Omega_{\Lambda,0} = 1$) can be found to be:

$$t_0 = \frac{H_0^{-1}}{3\sqrt{1-\Omega_{\mathrm{m},0}}} \ln\left(\frac{1+\sqrt{1-\Omega_{\mathrm{m},0}}}{1-\sqrt{1-\Omega_{\mathrm{m},0}}}\right). \tag{2.1.1}$$

In the absence of the cosmological constant ($\Omega_{\Lambda,0} \to 0$ or $\Omega_{\mathrm{m},0} \to 1$) we get:

$$t_0 = \frac{2}{3} H_0^{-1}. \tag{2.1.2}$$

Putting the value for the cosmological constant (through $h = 0.673$) we get:

$$t_0 = 9.6 \text{ Gyr} \tag{2.1.3}$$

But the age estimations of some old globular clusters of stars give ages larger than that, of the order of 13 Gyr. From the functional form of eq. (2.1.1), we see that the cosmic age increases as the matter density decreases (and thus the dark energy density increases).

2.2 Supernovae Type Ia

The first direct proof for an accelerating Universe and the presence of a cosmological constant came in 1998 with the observations of distant supernovae. In order to find out if the Universe is accelerating or decelerating you need to probe observational the change over time of the **expansion rate** of the Universe. In order to do so, you need to measure redshifts and distances to objects at the largest possible range. Measuring redshifts is easy – measuring distances is a little bit trickier! A way to determine distances is by using a class of objects with known intrinsic luminosities – known as **standard candles**. Then, the distance to these objects can be deduced by how bright they appear to be.

A class of such objects that can be thought of as standard candles (or, better, **standarizable** candles) are the Supernovae Type Ia (SN Ia) explosions. The term Ia is spectroscopic. A type I supernova does not include a hydrogen absorption line (as opposed to a SN of type II). Furthermore, if it contains an absorption line of singly ionized silicon, it is classified as type Ia. The interesting thing about this class of explosions is that it is believed that they are coming from a very special (and similar) physical process: the explosion of a white dwarf when reaches the Chandrasekhar limit ($\sim 1.4\ M_\odot$) as it accretes matter from a companion star. It is thus believed that the absolute luminosity of the explosion is constant and the

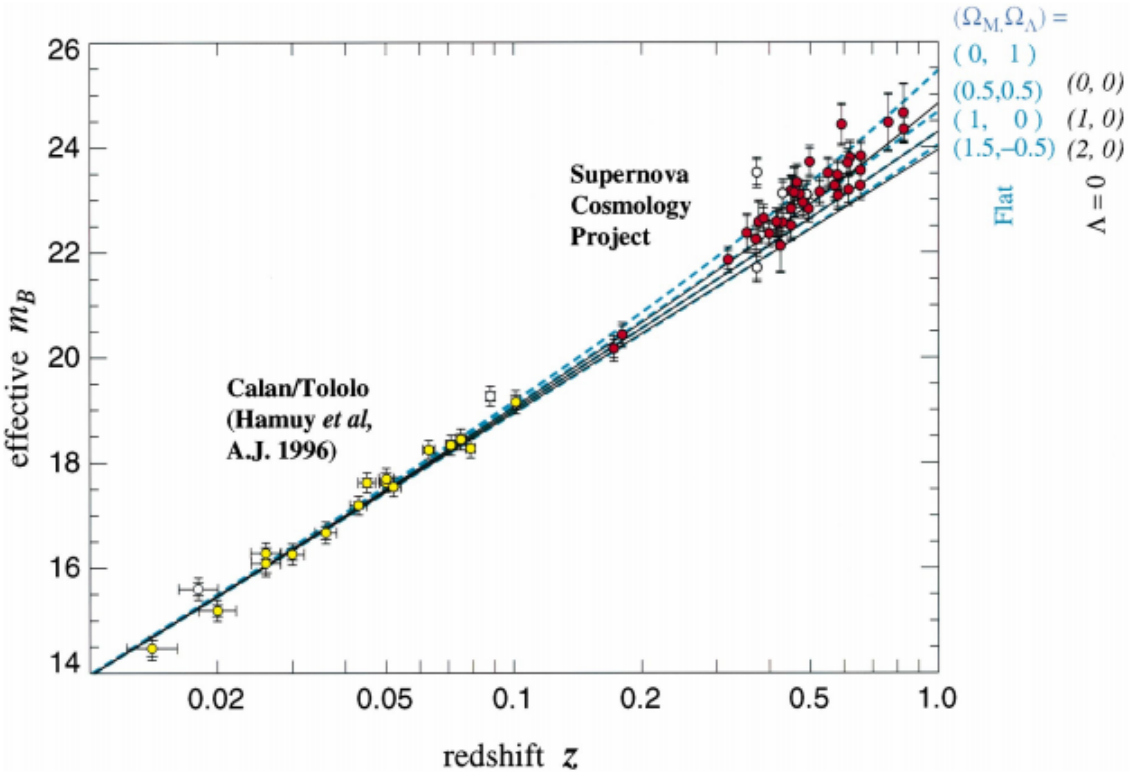

Figure 2.1: Apparent luminosity, m, versus redshift, z, for 42 high-z SN Ia and 18 low-z, from two different teams (see text). The appaerent luminosity, for a given redshift, predicted for different cosmologies is also plotted. The data are in favour of a Universe with a cosmological constant. Figure adapted from Perlmutter et. al. (1998), the original paper that demonstrated the accelerating expansion of the Universe and the existence of a cosmological constant.

same for all such explosions. Furthermore, the luminosity is very high and thus they can be used to measure great distances.

Indeed, there are complications and the above is a simplified picture. There is an intrinsic spread in in the absolute luminosities of supernovae Ia, due to the fact that thermonuclear reactions that trigger the explosions have not always the same efficiency. However they can be "normalized" since there is a correlation of the absolute luminosity with the light curve (the curve which shows how the brightness of a SN evolves with time). That is why we called SN as "standarizable" candles.

What we measure in Earth is the flux or the **apparent magnitude** of an object. Let us see how the apparent magnitude of a SN at a given redshift can be connected with the luminosity distance (see section 1.3) and thus with the particular cosmological model. For two objects with apparent fluxes F_1 and F_2 their apparent magnitudes m_1 and m_2 are related with the relationship:

$$m_1 - m_2 = -\frac{5}{2}\log_{10}\left(\frac{F_1}{F_2}\right). \tag{2.2.1}$$

The **absolute magnitude**, M, of an object is defined as the apparent magnitude it would have if it was placed at a distance of 10 pc. The apparent magnitude is

related to the absolute magnitude using the luminosity distance d_L:

$$m - M = 5 \log_{10} \left(\frac{d_L}{10\text{pc}} \right). \tag{2.2.2}$$

Expressing the luminosity distance in Mpc, the above equation becomes:

$$m - M = 5 \log_{10} d_L + 25. \tag{2.2.3}$$

From equation (1.3.8), the luminosity distance is:

$$d_L(z) = (1+z) \int_0^z \frac{dz'}{H(z')}. \tag{2.2.4}$$

Assuming a ΛCDM model, we have:

$$H(z) = H_0 \left[\Omega_{\text{m},0} (1+z)^3 + \Omega_{\Lambda,0} \right]^{1/2} \tag{2.2.5}$$

Assuming that $\Omega_{\text{m},0} + \Omega_{\Lambda,0} = 1$, we can express the luminosity distance as a function of the cosmological constant density parameter as:

$$d_L(z) = \frac{1+z}{H_0} \int_0^z \frac{dz'}{\left[(1 - \Omega_{\Lambda,0})(1+z')^3 + \Omega_{\Lambda,0} \right]^{1/2}}. \tag{2.2.6}$$

Since the absolute magnitude for all SN Ia is thought to be the same, then from eq. 1.3.8 we can relate the absolute magnitude with the luminosity distance and thus with cosmology. Figure 2.1 shows the diagram of apparent luminosity versus redshift for a number of SN Ia observations. There are measurements for 42 high-z SN Ia from the Supernova Cosmology Project and 18 low-z SN Ia from Calan/Tololo Supernova Survey. This figure is adapted from the original paper by Perlmutter et. al. (1998). In the same plot, theoretical predictions for the apparent magnitude in different cosmologies are presented. Solid lines correspond to cosmologies without dark energy: From top to bottom: $(\Omega_{\text{m},0}, \Omega_{\Lambda,0}) = (0,0), (1,0), (2,0)$. Dashed curves correspond to flat cosmologies, with (from top to bottom): $(\Omega_{\text{m},0}, \Omega_{\Lambda,0}) = (0,1), (0.5,0.5), (1,0), (1.5,0.5)$.

Data demonstrate that SN are fainter (so, they are more distant) compared even with a model of an empty universe (0,0). The best fit to the data is a cosmology with $(\Omega_{\text{m},0}, \Omega_{\Lambda,0}) \sim (0.3, 0.7)$.

2.3 CMB and Acoustic Oscillations

In the previous section we presented a standard candle method to determine distances and thus the expansion rate of the Universe. Now, we pass to a powerful **standard ruler** method, that is a method that uses the fact that a class of objects has known intrinsic size and thus the distance to them can be deduced by their apparent size.

We have already discussed the Cosmic Microwave Background and its oscillatory structure of the temperature anisotropies. As we will discuss now, there is an imprint of these primordial sound waves in the distribution of matter and galaxies in the late-time Universe. This phenomenon is known as **Baryon Acoustic Oscillations** (BAO's) and in a few words there is the existence of a preferred galaxy separation in this distribution of galaxies (see figure 2.2). The amplitude

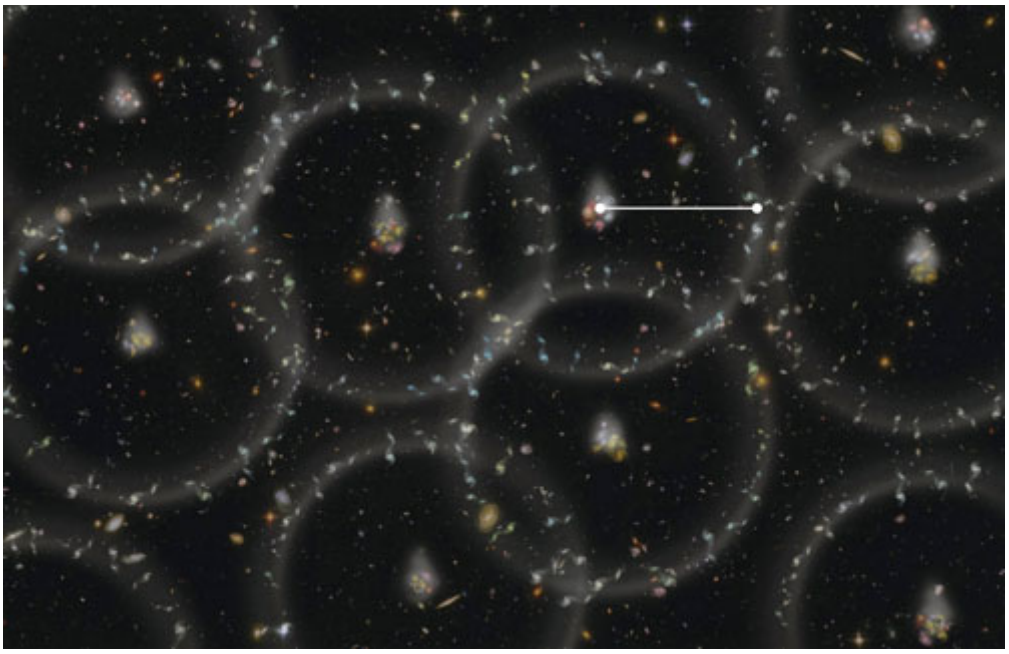

Figure 2.2: An exaggerated illustration of the BAO phenomenon

of this phenomenon is small (smaller than that of the CMB) and thus it presents a great statistical challenge.

The acoustic scale (the comoving size of the BAO) can be computed theoretically. It is the the distance the sound waves can travel from the Big Bang until recombination (in fact the size of the BAO is slightly bigger than that appeared on the CMB; after the CMB was emitted the sound waves continued to exist since there still were many more photons than baryons. Thus the BAO freeze epoch is at $z \sim 1060$, while the CMB release epoch is at $z \sim 1100$). The comoving scale of sound horizon/CMB is:

$$r_s = \int_0^{t_*} \frac{c_s(t)}{a(t)} dt = \int_{z_*}^{\infty} \frac{c_s(z)}{H(z)} dz \sim 150 \text{ Mpc}. \tag{2.3.1}$$

In the above expression c_s is the sound speed of the baryon-photon plasma, which has a maximum of about $c/\sqrt{3}$, c being the speed of light. z_* is the BAO freeze epoch, of $z \sim 1060$.

The size of the BAO feature is big and this has merits but also presents challenges. Being on large scales, it is not affected from astrophysical processes and non-linear structure formation. The scale of BAO can be theoretically determined with an accuracy better than 1%, making it an extremely reliable standard ruler.

Being on such large scales, on the other hand, it makes it challenging to detect since it requires the mapping of galaxy distribution on very large scales of the Universe. Furthermore, the signal is weak (less than 1% deviation from the homogeneity of the Universe), demands measurements of hundreds of thousands of galaxies, mapped in huge three dimensional volume in order for us to be able to detect.

Indeed measurements of the BAO feature has already been performed. In figure 2.3 we see the matter correlation function, plotted for different matter densities,

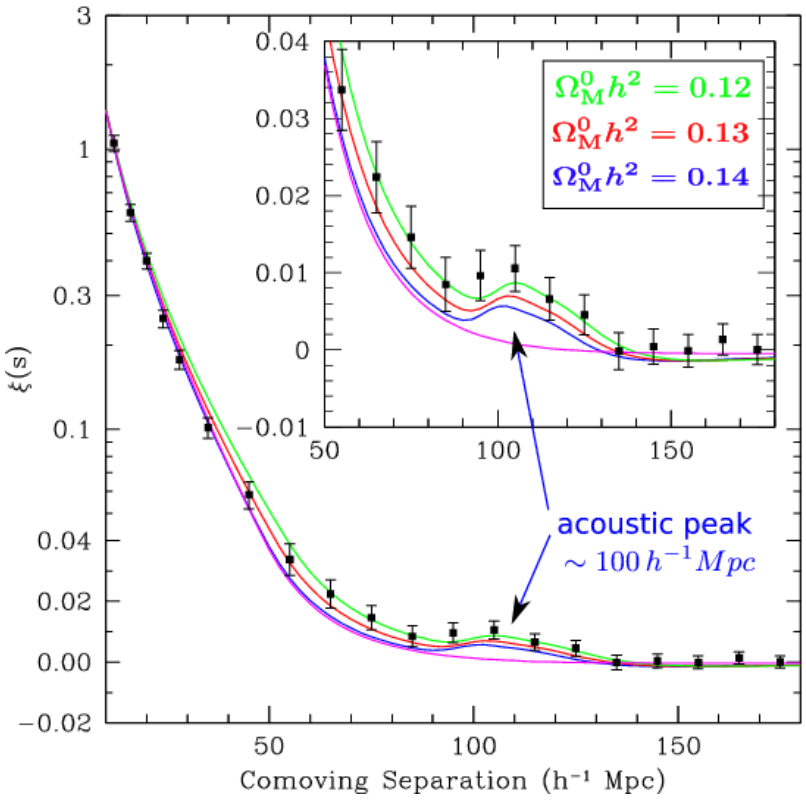

Figure 2.3: The matter correlation function and the BAO signal as a small pump at a comoving distance of $\sim 100\ h^{-1}$ Mpc

as well as the data points of the measurements (Eisenstein et. al. 2005). The BAO feature appears as a small bump in the correlation function. BAO method is a powerful tool, complementary to SN observations, in order to measure the expansion rate of the Universe.

2.4 Other Methods and the State of the Universe

We have presented the main methods we use in order to probe the accelerating expansion of the Universe and dark energy. Other techniques also exist, like galaxy cluster counts (measuring how the number density of galaxy clusters change over time), weak lensing and growth of cosmic structure. The use of the cosmic structure to probe dark energy is the main topic of this thesis and we will discuss it later in detail. We now note that the effect of a cosmological constant/dark energy on cosmic structure has to do with the fact that such a component acts anti-gravitational and halts structure growth.

Until now, the effect on structure formation has not been used extensively to probe precisely dark energy. This is mainly due to the lack of a good, robust observable quantity related to the cosmic structure depending on the values of the cosmological quantities.

Figure 2.4 shows the combined data from measurements of SN type Ia, Baryon Acoustic Oscillations and of the Cosmic Microwave Background (CMB). We see that observations of SN alone are insufficient to determine precisely the value of

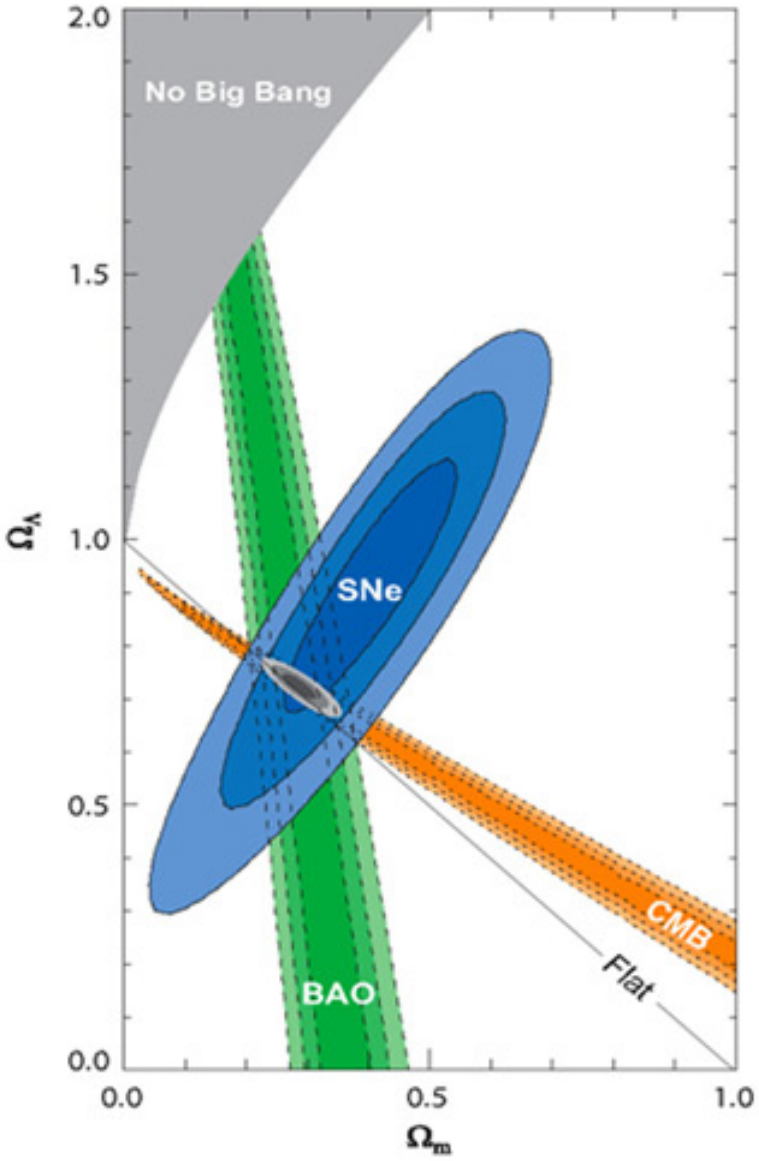

Figure 2.4: The combined data, pointing out to a flat Universe with matter and a cosmological constant.

the cosmological constant density. However, from CMB we have that the Universe must be flat which shrinks the range of possible values for the cosmological constant density. Combining also the data from BAO's (or from Galaxy Clusters) we constrain very well the matter and cosmological constant densities. The fact that three independent measurements agree and the three lines in figure 2.4 pass from the same point supports the concordance ΛCDM Universe, with parameters $\Omega_{m,0} \sim 0.3$ and $\Omega_{\Lambda,0} \sim 0.7$.

Chapter 3

Models of Dark Energy

In the present chapter we review the models proposed in order to explain the observational data pointing towards the existence of a dark energy component in the Universe. These include models that propose the existence of a real dark energy "substance" (like a cosmological constant or a scalar field that behaves like a dark energy with negative pressure), models that propose a modification of General Relativity at the largest scales and models that propose that the observations are not interpreted correct and that can be explained by assuming that we live in a special region of the Universe (void models) or that structure formation has effects on the apparent acceleration of the Universe (back-reaction models). We will discuss in quite detail the first class of models (cosmological constant and scalar field) since they are the most accepted and discussed models. Later we will study how the the turnaround radius (a concept that will explain in detail) of cosmic structures evolves with time in these models, and thus how it can be used to probe cosmology.

3.1 Cosmological Constant

The simplest solution to the problem of the presence of dark energy component in the Universe is to postulate the existence of a **cosmological constant**. A component that its energy density is constant in space and time. In fact, until now, all observations are in favour of this interpretation of dark energy. Although, as we will see, accepting this explanation makes cosmologists feel a little bit uncomfortable, for a number of reasons:

1. It does not provide a real "explanation" of the problem. You simply postulate the existence of another constant of Nature.

2. Cosmological constant can be thought as the zero-point vacuum energy of quantum fields. But from particle physics theories you expect a value for this vacuum energy many orders of magnitude larger than the observed.

3. It does not provide any explanation for the fine tuning and/or coincidence problem. That is, that its value is so small (and exactly as it should be for

structures to be able to form - this is connected to the **anthropic argument/principle**) and comparable to the matter density today.

In this section, we will discuss these issues, stating again that currently all observations point towards that dark energy behaves like a cosmological constant.

3.1.1 Introducing the Cosmological Constant in Einstein's Equations

Both sides of the Einstein's equations, eq. (1.1.5), obey the so-called relation:

$$G_{\mu\nu}{}^{;\nu} \equiv \left(R_{\mu\nu} - \frac{1}{2} R g_{\mu\nu} \right)^{;\nu} = 0, \qquad T_{\mu\nu}{}^{;\nu} = 0. \tag{3.1.1}$$

The first of them is known as the **Bianchi identity**, while the second expresses the conservation of energy and momentum. The metric also obeys a similar relation, $g_{\mu\nu}{}^{;\nu}$, so a term $\Lambda g_{\mu\nu}$ can be added to the left hand side of Einstein's equations:

$$R_{\mu\nu} - \frac{1}{2} R g_{\mu\nu} + \Lambda g_{\mu\nu} = 8\pi G T_{\mu\nu} \tag{3.1.2}$$

The left-hand side of the above equation is the most general local, coordinate-invariant, divergenceless, two-index tensor that can be constructed from the metric and its first and second derivatives. Note, that eq. (3.1.2) can be derived using the variational principle from the action:

$$S = \frac{1}{16\pi G} \int d^4x \sqrt{-g} \left(R - 2\Lambda \right), \tag{3.1.3}$$

where g is the determinant of the metric and R the Ricci scalar, of course. We will use actions and the variational principle later, when we will discuss scalar fields as dark energy candidates.

Using (3.1.2), we get the modified Friedmann and acceleration equations:

$$\left(\frac{\dot{a}}{a} \right)^2 = \frac{8\pi G}{3} + \frac{\Lambda}{3} - \frac{k}{a^2 R_0^2}, \tag{3.1.4}$$

and

$$\frac{\ddot{a}}{a} = -\frac{4\pi G}{3} \left(\rho + 3p \right) + \frac{\Lambda}{3}. \tag{3.1.5}$$

Eqs. (3.1.4) and (3.1.5) can be written in the form (1.1.10) and (1.1.11), if we define:

$$\rho_\Lambda \equiv \frac{\Lambda}{8\pi G}. \tag{3.1.6}$$

This is equivalent to moving $\Lambda g_{\mu\nu}$ to the right hand side and define the energy-momentum tensor of the vacuum as:

$$T_{\mu\nu}^{\text{vac}} = -\rho_{\text{vac}} g_{\mu\nu}, \tag{3.1.7}$$

with $\rho_{\text{vac}} g_{\mu\nu} = \rho_\Lambda$ as defined in (3.1.6). This describes a perfect fluid with $p = -\rho$, i.e. $w = -1$.

The cosmological constant as described in this subsection first introduced by A. Einstein, a little after he presented his field equations, in order to account for a **static Universe**. Back in his time, it was believed that the Universe was

static (not expanding or contracting). From (3.1.4) and (3.1.5) we see that a static solution is obtained (which means $\ddot{a} = \dot{a} = 0$) for a Universe containing pressureless matter ($p = 0$) and a cosmological constant, for:

$$\rho = \frac{\Lambda}{4\pi G}, \qquad \Lambda = \frac{k}{a^2 R_0^2}. \tag{3.1.8}$$

The solution though is unstable, since to achieve a static Universe the above eqs. must strictly hold. Indeed, when a few years after the introduction of the cosmological constant, astronomer Edwin Hubble discovered that the Universe is expanding, Einstein said that the introduction of the cosmological constant was "the biggest blunder he ever made in his life".

However, the idea of the cosmological constant was never totally abandoned. At any case, even when they thought that it was zero, there should be an explanation for this value. The cosmological constant returned in all its "glory" when the accelerated expansion of the Universe and remains with us ever since.

3.1.2 The Cosmological Constant Problem

The cosmological constant problem was a known problem even before the discovery of the accelerated expansion of the Universe (and thus the presence of a cosmological constant in the Universe). In this subsection we are going to discuss this problem, which remains one of the most important open questions in Physics and Cosmology.

The cosmological constant, as first introduced by Einstein, is a fudge quantity, a constant of nature that cannot be computed. However, from the particle physics/field theory point of view, the cosmological constant can be associated with the zero-point (vacuum) energy of quantum fields. Let us, for simplicity, consider just one scalar field, ϕ. The zero point energy of that field ($\hbar = c = 1$) for a mode of momentum k is:

$$E_k = \frac{\omega}{2} = \frac{1}{2}\sqrt{k^2 + m^2} \tag{3.1.9}$$

The zero-point (vacuum) energy of the field would thus be the sum of the zero-point energies of all modes:

$$\rho_{\rm vac} = \int \frac{d^3k}{(2\pi)^3} E_k = \int_0^\infty \frac{4\pi k^2 dk}{(2\pi)^3} \frac{1}{2}\sqrt{k^2 + m^2} = \infty \text{ !!!!} \tag{3.1.10}$$

We just found that the energy of the vacuum should be infinite! Ok, this is nonsense, of course. We are not sure that our theory (GR, Standard Model) is correct for very high energies. Thus we must introduce a cut-off energy scale, $k_{\rm max}$ (with $k_{\rm max} \gg m$) . Thus, we get for the vacuum energy:

$$\rho_{\rm vac} = \int \frac{d^3k}{(2\pi)^3} E_k = \int_0^{k_{\rm max}} \frac{4\pi k^2 dk}{(2\pi)^3} \frac{1}{2}\sqrt{k^2 + m^2} \cong \frac{k_{\rm max}^4}{16\pi^2}, \tag{3.1.11}$$

where in the integration we have used that $k_{\rm max} \gg m$, and that the integral is dominated by the large modes. What is the cut-off energy scale? We believe that the laws of physics we know are valid until the Planck scale:

$$m_{\rm Pl} \cong 10^{19} \text{ GeV}. \tag{3.1.12}$$

Putting this as the cut-off energy scale, from eq. (3.1.11) we find:

$$\rho_{\rm vac} \cong \frac{m_{\rm Pl}^4}{16\pi^2} \cong 10^{74}\ ({\rm GeV})^4. \tag{3.1.13}$$

However, the observed value of the vacuum energy (cosmological constant) is:

$$\rho_{\rm vac}^{\rm obs} \cong (10^{-3}\ {\rm eV})^4 \cong 10^{-48}\ ({\rm GeV})^4 \tag{3.1.14}$$

The old cosmological problem was that a large value for the vacuum energy was expected (eq. (3.1.13)), while it was believed that the vacuum energy was exactly zero. The new cosmological constant problem is the huge discrepancy between the expected and the observed value, compare eqs. (3.1.13) and (3.1.14):

$$\rho_{\rm vac}^{\rm obs} \cong 10^{-120}\rho_{\rm vac}^{\rm exp}. \tag{3.1.15}$$

There is a 120 orders of magnitude discrepancy! Is there any way to avoid (or, at least, soften) the problem? In Supersymmetry (SUSY), a theoretical extension to the Standard Model of Cosmology, not yet experimentally proven, for every Fermion field there is a Boson field counterpart, whose contributions to the zero-point vaccuum energy are opposite. However, if it exists, this symmetry is broken in lower energy (even at those energies currently explored in our accelerators). The typical energy scale of Supersymmetry is around $m_{\rm SUSY} = 10^3$ GeV. Taking this as the cut-off energy scale, we find:

$$\rho_{\rm vac}^{\rm SUSY} \cong 10^{12}\ ({\rm GeV})^4 \tag{3.1.16}$$

The discrepancy between this and the observed value is smaller, but still huge:

$$\rho_{\rm vac}^{\rm obs} \cong 10^{-60}\rho_{\rm vac}^{\rm SUSY}. \tag{3.1.17}$$

Although we can add a constant number (a cosmological constant) in our theory in order to reduce the vacuum energy down to the observed value, this explanation is not adequate and leads to **fine-tuning problems**.

3.1.3 The Coincidence Problem and the Anthropic Principle

As we have seen in the previous chapter, the observations suggest that the current energy densities (density parameters) of the matter and dark energy (suppose for the time that it is a cosmological constant indeed) are:

$$\Omega_{\rm m,0} \cong 0.30, \tag{3.1.18}$$

and

$$\Omega_{\Lambda,0} \cong 0.70. \tag{3.1.19}$$

The two densities are of the same order of magnitude today. This is unexpected, since the ratio of these two quantities changes as:

$$\frac{\Omega_\Lambda}{\Omega_{\rm m}} = \frac{\rho_\Lambda}{\rho_{\rm m}} \propto a^3. \tag{3.1.20}$$

Thus, the two quantities are comparable (and thus we would be able to see the transition from matter to dark energy domination) for a very short time interval in cosmic time.

It seems odd that we are living exactly in such an epoch, this is another **fine-tuning** or coincidence problem. Proposals to solve this include a dark energy (not cosmological constant) that responds to the trend of ρ_m, models with several epochs of acceleration (such that seeing now an acceleration is not something "special") or that cosmic acceleration is backreaction of the growth of structure.

Connected to the fine-tuning and the coincidence problems is the **Anthropic Principle**. The Anthropic Principle comes in two variants:

1. The Strong Anthropic Principle (SAP), which states that the Universe, the physical laws and the values of the physical constants are properly adjusted in order that observers can be created.

2. The Weak Anthropic Principle (WAP), which states that since we are here as observers of the Universe the physical laws and the values of the physical constants must be compatible to that fact.

Although the Strong Anthropic Principle is closer to philosophy or even theology than science, the Weak Anthropic Principle can give an insight to the range of allowed values of physical constants. Applying it for the case of the Cosmological Constant, requiring that it must allow cosmic structures to form, Weinberg computed an allowed range:

$$-10^{-123}\ m_{\rm Pl}^4 <\approx \rho_\Lambda <\approx 3\times 10^{-121}\ m_{\rm Pl}^4. \tag{3.1.21}$$

The range was computed well before the observations of the accelerated Universe however it encloses the observationally obtained value!

3.2 Scalar Field Models of Dark Energy

In the present section we will discuss a large class of models that the presence of a evolving scalar field, ϕ, can act as a dark energy component, with equation of state parameter $w < -1/3$. Unlike the cosmological constant, the equation of state of these models can change with time, probably on timescales comparable to –or even smaller– than the age of the Universe. Models producing an equation of state $w \geq -1$ are referred to as **quintessence**, while models resulting to a equation of state $w \leq -1$ are known as **phantom models**. There are also models where the equation of state is crossing the cosmological constant barrier ($w = -1$) from above to below, or oppositely (**quintom scenario**). Other models as **k-essence** are also viable. Although some of these models have theoretical problems (like stability), they have phenomenologically rich properties and it is possible to give insight to the nature of dark energy. In the next chapter, we will discuss how the evolution of cosmic structures can be used to probe the equation of state of dark energy and thus the above models.

3.2.1 Quintessence

The most explored scalar field dark energy models are these involving a scalar field, ϕ, with canonical kinetic energy and a potential $V(\phi)$, that interacts with the other components of the Universe only gravitationally. These are known as **quintessence models** and as we have said give an equation of state $w \geq -1$

(and we are going to demonstrate this). Scalar fields are good candidates for dark energy. The mean value of the field can have negative pressure, even if a gas consisting of the particles corresponding to the field does not. They are also simple since they contain no internal degrees of freedom (the only d.o.f is the potential).

The Lagrangian density of the scalar field is:

$$\mathcal{L}_\phi = -\frac{1}{2} g^{\mu\nu} \partial_\mu \phi \partial_\nu \phi - V(\phi) \tag{3.2.1}$$

The action that describes the theory (Gravitation + the scalar field) is:

$$S = \int d^4x \sqrt{-g} \left[\frac{1}{16\pi G} R + \mathcal{L}_\phi \right] + S_{\rm m}, \tag{3.2.2}$$

with R the Ricci scalar, as usual, and $S_{\rm m}$ the matter action. Also:

$$g \equiv \det g_{\mu\nu}, \tag{3.2.3}$$

the determinant of the metric. In the way we have written the action, the scalar field is minimally coupled to gravity, in the sense that the Lagrangian of the scalar field is multiplied only with the determinant of the metric and not with higher derivatives of it.

Varying the action (3.2.2) with respect to ϕ, we get the Euler-Lagrange equation:

$$\frac{\partial \left(\sqrt{-g} \mathcal{L}_\phi \right)}{\partial \phi} - \partial_\mu \frac{\partial \left(\sqrt{-g} \mathcal{L}_\phi \right)}{\partial \left[\partial_\mu \phi \right]} = 0. \tag{3.2.4}$$

For the Lagrangian density (3.2.1) this becomes:

$$-\frac{1}{\sqrt{-g}} \partial_\mu \left(\sqrt{-g} g^{\mu\nu} \partial_\nu \phi \right) + V'(\phi) = 0, \tag{3.2.5}$$

where we have defined:

$$V'(\phi) \equiv \frac{dV(\phi)}{d\phi}. \tag{3.2.6}$$

Now, for the spatially flat FRW metric in Cartesian coordinates we have (compare with eq. (1.1.7) – for convenience we have also set $R_0 = 1$):

$$g^{\mu\nu} = \mathrm{diag}\left(-1, a^{-2}, a^{-2}, a^{-2} \right). \tag{3.2.7}$$

Thus $g = \det g_{\mu\nu} = -a^6 \ \Rightarrow \sqrt{-g} = a^3$. The equation of motion of the scalar field thus becomes:

$$\begin{aligned} -a^{-3} \partial_\mu \left(a^3 g^{\mu\nu} \partial_\nu \phi \right) + V' &= 0 \Rightarrow \\ \Rightarrow -a^{-3} \partial_0 \left(a^3 g^{00} \partial_0 \phi \right) - a^{-3} \partial_i \left(a^3 g^{ii} \partial_i \phi \right) + V' &= 0 \Rightarrow \\ \Rightarrow 3a^{-3} a^2 \dot{a} \dot{\phi} + \ddot{\phi} - a^{-2} \nabla^2 \phi + V' &= 0. \end{aligned}$$

With the definition of the Hubble parameter, $H \equiv \frac{\dot{a}}{a}$, and assuming that the field is almost homogeneous ($\partial_i \phi = 0$) we finally get:

$$\boxed{\ddot{\phi} + 3H\dot{\phi} + V'(\phi) = 0.} \tag{3.2.8}$$

From the Lagrangian, we can also get the energy-momentum tensor for quintessence:

$$T^{\phi}_{\mu\nu} = -\frac{2}{\sqrt{-g}}\frac{\delta\left(\sqrt{-g}\mathcal{L}_{\phi}\right)}{\delta g^{\mu\nu}}. \tag{3.2.9}$$

For the Lagrangian density (3.2.1), we get:

$$T^{\phi}_{\mu\nu} = \partial_{\mu}\phi\partial_{\nu}\phi - g_{\mu\nu}\left(\frac{1}{2}g^{\alpha\beta}\partial_{\alpha}\phi\partial_{\beta}\phi + V\right). \tag{3.2.10}$$

The energy density and momentum are given in terms of the energy-momentum tensor components:

$$\rho = -T^{0}{}_{0}{}^{\phi}, \qquad p = T^{i}{}_{i}{}^{\phi}, \tag{3.2.11}$$

where in the second relation, the Einstein summation convention is **not** used. Working for a flat FRW metric, as before, we get for the **energy density**:

$$\begin{aligned}
\rho = -T^{0}{}_{0}{}^{\phi} &= \dot{\phi}^2 + \left(\frac{1}{2}g^{\alpha\beta}\partial_{\alpha}\phi\partial_{\beta}\phi + V\right) \\
&= \dot{\phi}^2 + \frac{1}{2}\underbrace{g^{00}}_{=-1} + \frac{1}{2}g^{ii}\underbrace{\partial_i\phi}_{=0}\underbrace{\partial_i\phi}_{=0} + V \\
&= \dot{\phi}^2 - \frac{1}{2}\dot{\phi}^2 + V,
\end{aligned}$$

where in the second line we have used that the scalar field is homogeneous and thus $\partial_i\phi = 0$. So, finally we have:

$$\boxed{\rho = \frac{1}{2}\dot{\phi}^2 + V.} \tag{3.2.12}$$

and the **momentum**:

$$\begin{aligned}
p = T^{i}{}_{i}{}^{\phi} &= \partial^{i}\phi\partial_{i}\phi - g_{ii}\left(\frac{1}{2}g^{\alpha\beta}\partial_{\alpha}\phi\partial_{\beta}\phi + V\right) \\
&= -a^2\left(\frac{1}{2}(-1)\dot{\phi}^2 + \frac{1}{2}a^{-2}\underbrace{\partial_i\phi\partial_i\phi}_{=0} + V\right) \\
&= \frac{1}{2}\dot{\phi}^2 - V,
\end{aligned}$$

so:

$$\boxed{p = \frac{1}{2}\dot{\phi}^2 - V.} \tag{3.2.13}$$

As we can see, the field has negative pressure when the potential dominates over the kinetic term, i.e. when the field is moving slowly.

The equation of state parameter $w = p/\rho$ is then:

$$\boxed{w = \frac{\dot{\phi}^2 - 2V(\phi)}{\dot{\phi}^2 + 2V(\phi)} = \frac{1 - 2V(\phi)/\dot{\phi}^2}{1 + 2V(\phi)/\dot{\phi}^2}.} \tag{3.2.14}$$

From the above equation is clear that this model gives $-1 \leq w \leq 1$. If the kinetic term, $\frac{1}{2}\dot{\phi}^2$ dominates, then $w \cong 1$. If the potential term $V(\phi)$ dominates then $w \cong -1$. For the condition of ϕ acting as a dark energy component that caused the cosmic acceleration, i.e. the equation of state to be $w < -1/3$, to be realized it must hold the condition $\dot{\phi}^2 < V(\phi)$.

If the potential have a sufficiently flat shape the field evolves slowly along it. From eq. (3.2.8) we see that the friction term $(3H\dot{\phi})$ will slow down the field (that is, to make $\dot{\phi}$ small enough to satisfy the above condition, even if it was not satisfied initially).

The Friedmann equation in a flat Universe where the scalar field is the dominant component can be written as:

$$H^2 = \frac{8\pi G}{3}\rho = \frac{1}{3m_{\rm pl}^2}\rho = \frac{1}{3m_{\rm Pl}^2}\left[\frac{1}{2}\dot{\phi}^2 + V(\phi)\right], \tag{3.2.15}$$

where we have defined the **Planck mass**:

$$m_{\rm Pl} \equiv \frac{1}{\sqrt{8\pi G}}, \qquad (\hbar = c = 1). \tag{3.2.16}$$

The conditions for the field to **slow roll** are then:

$$\dot{\phi}^2 \ll V, \qquad |\ddot{\phi}| \ll 3H|\dot{\phi}|. \tag{3.2.17}$$

If the above conditions are valid, we can approximate eqs. (3.2.8),(3.2.16) as:

$$3H\dot{\phi} = -V', \qquad H^2 = \frac{V}{3m_{\rm Pl}^2}. \tag{3.2.18}$$

We introduce now two very important parameters, known as **slow-roll parameters**:

$$\epsilon(\phi) \equiv \frac{1}{2}m_{\rm Pl}^2\left(\frac{V'}{V}\right)^2 \tag{3.2.19}$$

and

$$\eta(\phi) \equiv m_{\rm Pl}^2\frac{V''}{V}, \tag{3.2.20}$$

where we have also defined $V'' \equiv \frac{d^2V}{d\phi^2}$. If the slow-roll parameters are very small, $\epsilon \ll 1$ and $|\eta| \ll 1$, then the slow-roll conditions are satisfied.

It is interesting to note that, although the above discussion is given in the content of the quintessence model, trying to explain the late-time acceleration of the Universe, this discussion is identical to that of the **inflaton field**, that it is supposed to be responsible for an initial rapid expansion of the Universe, called **cosmological inflation**.

The specific quintessence model is described through its particular potential. There are many models, that can generally be classified in two broad categories. First are the **freezing models**, with representative potentials:

$$V(\phi) = M^{4+n}\phi^{-n}, \quad (n > 0) \tag{3.2.21}$$

$$V(\phi) = M^{4+n}\phi^{-n}\exp\left(a\phi^2/m_{\rm Pl}^2\right) \tag{3.2.22}$$

In this class, the field in the past was rolling along the potential, but the movement gradually slows down after the system enters the phase of cosmic acceleration.

There are also the **thawing models**, with representative potentials:

$$V(\phi) = V_0 + M^{4-n}\phi^n \quad (3.2.23)$$

$$V(\phi) = M^4 \cos^2(\phi/f) \quad (3.2.24)$$

In those models, the field, which has mass m_ϕ, has been frozen until recently (and thus it had $w \cong -1$ at early times) and then begins to evolve at the time when H drops below m_ϕ.

3.2.2 Phantom Energy

Although quintessence gives an equation of state parameter $w \geq -1$, **phantom energy** has the property that it has an equation of state parameter $w \leq -1$. The simplest way to obtain such a phantom component is to consider a scalar field ϕ with negative kinetic (and gradient, if it is not homogeneous) energy.

The Lagrangian of such a model would be (compare with eq. (3.2.1)):

$$\mathcal{L}_\phi = \frac{1}{2} g^{\mu\nu}\partial_\mu\phi\partial_\nu\phi - V(\phi). \quad (3.2.25)$$

As you can see, the canonical term now has its sign reversed, compared to the Lagrangian of quintessence. Working again in a flat FRW metric, $ds^2 = -dt^2 + a^2(t)[dx^2 + dy^2 + dz^2]$, we get the equation of motion of the field:

$$\ddot{\phi} + 3H\dot{\phi} - a^{-2}\nabla^2\phi - V'(\phi) = 0. \quad (3.2.26)$$

Assuming the field homogeneous, $\partial_i\phi = 0$ and the equation of motion of the field reduces to:

$$\ddot{\phi} + 3H\dot{\phi} - V'(\phi) = 0. \quad (3.2.27)$$

Note that scalar fields with negative kinetic terms, as opposed to those with positive, evolve to the maxima of their potential. Working as in the case of quintessence, we get the **energy density** of the phantom field:

$$\rho = -\frac{1}{2}\dot{\phi}^2 + V(\phi), \quad (3.2.28)$$

and its **pressure**:

$$p = -\frac{1}{2}\dot{\phi}^2 - V(\phi). \quad (3.2.29)$$

The resulting **equation of state** parameter is then:

$$\boxed{w = \frac{p}{\rho} = \frac{\dot{\phi}^2 + 2V(\phi)}{\dot{\phi}^2 - V(\phi)}.} \quad (3.2.30)$$

From the above equation it is clear that the equation of state satisfies $w \leq -1$.

Although the model seems simple and well-defined it has serious stability problems. If we allow fluctuation in this field, these will have a negative energy and thus it will be energetically preferred for it to decay in positive-energy and negative-energy particles. If this happens in timescales compared to, or less than, the age of the Universe the model can't be true. Generally, the phantom field, if it exists cannot be consider fundamental, but rather an effective low-energy description of physics active in higher energies.

3.2.3 K-essence, Quintom and Time Variation of the EoS

k-essence

There also exist more complicated scalar field models than those discussed so far. A broad class is that of scalar fields, ϕ, with non-canonical kinetic terms. Defining the **kinetic-term variable**:

$$X \equiv -\frac{1}{2} g^{\mu\nu} \partial_\mu \phi \partial_\nu \phi, \tag{3.2.31}$$

we can write the action of the scalar field as:

$$S_\phi = \int d^4x \sqrt{-g} P(X, \phi), \tag{3.2.32}$$

with P a general function of the kinetic-term variable, X and the field, ϕ. Working as before we get the energy density and the pressure of the field:

$$\rho = 2X \frac{\partial P}{\partial X} = 2X P_{,X}, \tag{3.2.33}$$

where we have defined $P_{,X} \equiv \frac{\partial P}{\partial X}$ and

$$p = P(X, \phi) \tag{3.2.34}$$

resulting in an equation of state:

$$w = \frac{p}{\rho} = \frac{P}{2XP_{,X} - P} = -1 + \frac{2XP_{,X}}{2XP_{,X} - P}. \tag{3.2.35}$$

Demanding the energy density to be positive $\rho = 2X \frac{\partial P}{\partial X} = 2XP_{,X} > 0$, we see that equation of state can be either be $w \geq -1$ or $w \leq -1$, but without crossing the cosmological constant ($w = -1$) barrier.

Quintom scenario

There remains the possibility that the equation of state parameter neither is constant in time, no it always remain in the $w \leq -1$ or $w \geq -1$ regime, but rather it crosses the cosmological constant boundary ($w = -1$) at a particular epoch.

All models we have seen so far do not have this property; they produce equations of state that always remain on either side of the boundary. It can be shown that it cannot produce a viable **quintom model** (quintom, from quint(essence) and (phant)om) with only one scalar field. Extra degrees of freedom are needed (or a non-minimal coupling to gravity).

A simple quintom model can be constructed by considering a quintessential scalar field, ϕ, and one phantom scalar field, σ. The action that describes the total model (including gravity and the matter section) is:

$$S = \int d^4x \sqrt{-g} \left[\frac{1}{16\pi G} R - \frac{1}{2} g^{\mu\nu} \partial_\mu \phi \partial_\nu \phi - V_\phi(\phi) + \frac{1}{2} g^{\mu\nu} \partial_\mu \sigma \partial_\nu \sigma - V_\sigma(\sigma) \right] + S_{\mathrm{m}}, \tag{3.2.36}$$

where we have used subscripts to denote that the potentials of the two fields have not (of course) the same functional form. It comes of no surprise that the energy densities and pressures of the two fields are:

$$\rho_\phi = \frac{1}{2}\dot{\phi}^2 + V_\phi(\phi), \qquad p_\phi = \frac{1}{2}\dot{\phi}^2 - V_\phi(\phi), \tag{3.2.37}$$

and

$$\rho_\sigma = -\frac{1}{2}\dot{\sigma}^2 + V_\sigma(\sigma), \qquad p_\sigma = -\frac{1}{2}\dot{\sigma}^2 - V_\sigma(\sigma), \tag{3.2.38}$$

and the equations of motion of the fields are:

$$\ddot{\phi} + 3H\dot{\phi} + \frac{\partial V_\phi(\phi)}{\partial \phi} = 0, \tag{3.2.39}$$

$$\ddot{\sigma} + 3H\dot{\sigma} - \frac{\partial V_\sigma(\sigma)}{\partial \sigma} = 0. \tag{3.2.40}$$

$$\tag{3.2.41}$$

Defining as the dark energy the combination of the two fields, then:

$$\rho_{\rm de} = \rho_\phi + \rho_\sigma, \qquad p_{\rm de} = p_\rho + p_\sigma. \tag{3.2.42}$$

The equation of state of dark energy is then defined as:

$$w_{\rm de} = \frac{\rho_{\rm de}}{p_{\rm de}} = \frac{\rho_\phi + \rho_\sigma}{p_\phi + p_\sigma} \tag{3.2.43}$$

It depends on which of the two fields dominate, if we have $w \leq -1$ or $w \geq -1$.

Time evolution of the equation of state

As we have seen, the time evolution of the equation of state parameter is allowed, in which case we do not have a constant w but rather an equation of state that is a function of cosmic time, $w(a)$, where a is the scale factor of the Universe.

Although the functional form of $w(a)$ may be complicated and different for different dark energy models, it can be approximated with an expansion around the present epoch. There are many such **parametrizations**, that are usually make use of two parameters. One very common parametrization is the $\{w_0, w_a\}$ parametrization:

$$w(a) = w_0 + (1-a)w_a. \tag{3.2.44}$$

The present day value is w_0, while the derivative $dw/da = -w_a$. With this parametrization the density of dark energy scales as:

$$\rho_{\rm de} = \rho_{\rm de,0} \exp\left(3\int_a^1 \frac{1+w(a')}{a'}da'\right) = \rho_{\rm de,0} a^{-3(1+w_0+w_a)} \exp\left[-3w_a(1-a)\right]. \tag{3.2.45}$$

There also exist other parametrizations, as for example the $\{w_0, w_1\}$ parametrization:

$$w(a) = w_0 + w_1 a(1-a), \tag{3.2.46}$$

which has also has a present day value of w_0 but its derivative is now $dw(a)/da = w_1(1-2a)$.

3.3 Modified Gravity

Until now we have tried to explain the dark energy in the Universe (beyond the naive introduction of a cosmological constant) by introducing extra degrees of freedom in the form of scalar fields. That is, to modify the right hand side of the Einstein equations, i.e., to introduce in the Energy momentum tensor a component different from ordinary matter.

It is profound that, in order to explain cosmic acceleration and the presence of "dark energy", you can also think of modifying the left-hand side of Einstein's equations. These models are collectively known as **modified gravity models**. The detailed description of those models is beyond the scope of this thesis, so we will only mention the main points.

Note that any modification of Einstein's equations can be interpreted as standard gravity with a modified "matter source", containing a mixture of scalars, vectors and tensors. However, in the present section we are interested in explicit modified gravity models, where the left hand side of Einstein's equations are modified.

Standard gravity (and the models we have encounter so far) arises from the Einstein-Hilbert action:

$$S = \frac{1}{16\pi G}\int d^4x\sqrt{-g}R + S_{\rm m}, \tag{3.3.1}$$

where in the $S_{\rm m}$ we have encompassed the matter terms, as well as any dark energy component coming from a cosmological constant or a scalar field. A class of modified gravity models is the $f(R)$ gravity, where the action is given from a generic function of the Ricci scalar R:

$$S = \frac{1}{16\pi G}\int d^4x\sqrt{-g}f(R) + S_{\rm m}. \tag{3.3.2}$$

The functional form of $f(R)$ must be such that it will reproduce the observed late-time acceleration of the Universe. This means a modification of gravity for small values of R (a modification where the curvature is small, i.e. the largest scales of the Universe).

A number of models have been proposed, chosen as to satisfy some very specific conditions. For example, in order to avoid a negative effective gravitational constant, the model must have $f_{,R} > 0$ for $R \geq R_0$, where R_0 is the present-day Ricci scalar. Also it must hold that $f(R) \to R - 2\Lambda$ for $R \gg R_0$ to be consistent with local gravity tests. Other, more technical conditions, also exist. Models that have been proposed and satisfy them, include:

$$f(R) = R - \mu R_c\left(\frac{R}{R_c}\right)^p, \qquad \text{with } 0 < p < 1,\ \mu, R_c > 0, \tag{3.3.3}$$

$$f(R) = R - \mu R_c\left[1 - \left(1 + \frac{R^2}{R_c^2}\right)^{-n}\right], \qquad \text{with } n, \mu, R_c > 0 \tag{3.3.4}$$

$$f(R) = R - \mu R_c\frac{(R/R)^{2n}}{(R/R_c)^{2n} + 1}, \qquad \text{with } n, \mu, R_c > 0 \tag{3.3.5}$$

$$f(R) = R - \mu R_c\tanh\left(\frac{R}{R_c}\right), \qquad \text{with } \mu, R_c > 0. \tag{3.3.6}$$

There are also more complicated models, such as **scalar-tensor theories**, where gravity induced not only from a tensor field, but also from a scalar one:

$$S = \int d^4x\sqrt{-g}\left[\frac{1}{2}f(\phi, R) - \frac{1}{2}\zeta(\phi)(\partial\phi)^2\right] + S_{\rm m}, \tag{3.3.7}$$

where f is a general function of the scalar field ϕ and the Ricci scalar, R, and ζ a function of the scalar field.

Other classes of theories also exist, like the DGP (Dvali-Gabadadze-Porrati) model, motivated by string theory , Gauss-Bonnet dark energy models, Galileons, Chameleons etc. The list is very long, indeed.

3.4 Inhomogeneous Cosmological Models

So far we have tried to explain cosmic acceleration, as this is inferred from observations of distant supernovae, for example, by introducing new physics. These included the presence of a cosmological constant, the act of scalar fields or the modification of the General Theory of Relativity. However, it is conceivable that data point out to the breakdown of another pillar of modern cosmology: the **cosmological principle**, which states that theere is no preferred position or direction in the Universe, and we live in a typical part of it.

A proposal for the explanation of cosmic acceleration without involving a "dark" sector, is that we live near the center of a giant **cosmic void**. A void is a large underdensity; thus it expands faster than the mean of the Universe. Living near its center would mimic the effects (in expansion rate) of a cosmological constant. Its radius should be a far as $z \cong 0.3 - 0.5$, to be compatible with observations.

To describe formally the time evolution of that huge spherical inhomogeneity, we must abandon the FRW metric and make use of the Lemaitre-Tolman-Bondi (LTB):

$$ds^2 = -dt^2 + \frac{(R')^2}{1+2E}dr^2 + R^2\left(d\theta^2 + \sin^2\theta d\phi^2\right)^2, \tag{3.4.1}$$

$$R = R(t, r), \qquad R' = \partial R/\partial r, \qquad E = E(r)(> -1/2). \tag{3.4.2}$$

The arbitrary function of the comoving coordinate r, $E(r)$, is like a position-dependent spatial curvature. The parametric solution of the emergent Einstein equations fo $E > 0$ (the case we are interested in) is:

$$R = \frac{M}{2E}(\cosh\eta - 1), \qquad (\sinh\eta - \eta) = \frac{(2E)^{3/2}(t - t_B)}{M}, \tag{3.4.3}$$

where t_B is the "Big Bang Time", i.e. the the time when $\eta, R = 0$ for a point with comoving coordinate r.

We are not going to discuss further this model. It is a model that has attracted some attention but the notion of living in a very special position at the center of a very special void seems to produce a more severe "fine tuning problem" than the one it tries to solve. It also seems to have problems in interpreting observational data.

Other inhomogeneous models discussed are those that think of the cosmic acceleration as a back reaction of the effect of local inhomogeneities. To put it

simple, that the metric of the Universe is the average on very large scales of the full complicated metric that describes the Universe at all its detail and inhomogeneity. And that this averaged metric can lead to correction terms (compared to the ordinary FRW metric) that can mimic the effect of the cosmological constant.

Chapter 4

Probing Dark Energy at Turnaround I: Theory

In the present chapter we propose a new **local** cosmological test/probe for dark energy, which is based on its effect of cosmic structures. We start by discussing qualitative this new cosmological probe, focusing on the concept of **turnaround radius** radius and how cosmological parameters are imprinted in its time evolution. We propose it as the optimum observable if we want to use cosmic structure in order to probe dark energy. The calculation of the evolution of the turnaround radius passes through the calculation of the **turnaround overdensity**, the overdensity (which depends on time) a region of the Universe must have for turnaround a given time. This can be calculated using the simple **spherical collapse model**. We show how to use that model in order to calculate the turnaround overdensity in different cosmologies (matter only, ΛCDM, clustering and homogeneous dark energy). In the following chapter we will use these results to show that it is in principle possible to extract information about the cosmological parameters $(\Omega_{\mathrm{m},0}, \Omega_{\Lambda,0}, w)$ by demonstrating that different cosmological models produce distinct evolution histories of the turnaround radius.

4.1 A New Cosmological Probe

As we have seen (Chapter 2), the existence of a dark energy component in the matter-energy content of the Universe is now supported by a diverse set of observations . All current observations are consistent with the simplest possible candidate, a cosmological constant Λ, whose density remains constant in time. The most explored alternative is a dark energy component with an equation of state parameter $w \neq -1$. However, more exotic alternatives are also pursued, including living in a giant cosmic void that leads to an apparent global acceleration, or deviations from General Relativity at the largest scales (see Chapter 3).

Although observations pointing towards the existence of dark energy vary in nature, they all share a common feature: they all consider the Universe at its largest scales, by measuring, for example, its –apparently– accelerated expansion through observations of distant supernovae or by tracing the discrepancy between the measured matter density of the Universe and the energy density needed for the Universe to be flat as a whole, as CMB observations indicate . It may still thus be

possible that the above are just manifestations of our ignorance of physics at the largest scales. For this reason, a "local" test probing the existence of dark energy would be a powerful complement to our observational cosmology tool arsenal, in order to check for consistency results obtained using the above methods.

A dark energy component in the form of a cosmological constant has a prominent effect on the process of structure formation: acting "anti-gravitationally", it halts structure growth. In such a cosmology, a clear prediction can be made of the maximum turnaround radius –the non-expanding shell furthest away from the center of a bound structure (see the following section)– a cosmic structure can have. In (Pavlidou & Tomaras, 2014) it is shown that this maximum value for a structure of mass M is equal to:

$$R_{\rm ta,max} = \left(\frac{3GM}{\Lambda c^2}\right)^{1/3}, \tag{4.1.1}$$

where G is Newton's gravitational constant and c is the speed of light. This requirement can be used to construct cosmological test, which is to find **non-expanding** structures with radii violating the bound (4.1.1).

Even though this test is extremely powerful and robust, in its simplest form it is not flexible enough to provide constraints on the cosmological parameters. Rather, if the Universe is indeed ΛCDM, it can only provide a null result; if not, it can point to the need of a different cosmological model. In the present work, we overcome this shortcoming by extending the ΛCDM predictions of the turnaround radius of structures beyond that infinite time in the future (corresponding to the maximum value, eq. (4.1.1)): rather, we present a prediction for every cosmic epoch and for any possible combination of $\Omega_{\rm m,0}$ and $\Omega_{\Lambda,0}$.

In this and in the following chapter, our aim is to demonstrate that it is **in principle** possible to use measurements of turnaround masses and radii of structures, at different epochs, in order to determine the values of $\Omega_{\rm m,0}$ and $\Omega_{\Lambda,0}$. Particularly, we show that it is possible to construct a new test that can prove that a non-zero cosmological constant exists, using **local** physics –not concerning the Universe as a whole. Such a proof –if verified– would present an extreme challenge for more exotic alternatives to dark energy, such as those described above. On the other hand, a difficulty to firmly detect a $\Lambda \neq 0$ using this method, would constitute a strong indication of physics beyond ΛCDM. In both cases, we would have an extremely important result. This work gives a "proof of principle" for the feasibility of such a test.

Then, we extend our discussion for the case of a general dark energy component –with a constant equation of state parameter w– for the cases where the dark energy is clustering or homogeneous. We demonstrate that in the for quintessence models it is possible to gain information about the equation of state parameter with measurements in the present epoch. We present preliminary results for the case of a homogeneous phantom energy. In the following chapter we discuss possible extensions to our method.

4.2 The Turnaround Radius: Qualitative Discussion

What is the turnaround radius? Let us discuss qualitatively the spherical collapse model. The spherical collapse model gives insight to the complex process

of structure formation although makes some extremely simplifying assumptions. This model considers an initial, spherical, homogeneous and isotropic perturbation which evolves in a background Universe.

The perturbation starts following the expansion of the background Universe. However, since it has a higher matter density than the average, its expansion rate will slow down compared to the background. The perturbation will reach a maximum size before starting a process of contraction. The radius of the perturbation at the point of maximum size is known as the **turnaround radius**. After that point structure contracts. In view of this simple model, its ultimate fate is to become a singularity. Indeed, since perfect homogeneity and isotropy is just a simplification, dirty physics take action, and the perturbation collapses to a bound structure where the virial theorem is obeyed. A **virialized structure**. The corresponding radius is known as the virial radius.

In a Universe that contains a dark energy component, an anti-gravity, that affects the turnaround radius; not every initial perturbation is able to overcome the effect of it. In the ΛCDM universe there is a maximum size for the turnaround radius of a structure, eq. (4.1.1).

Studying structure formation and designing a cosmological test at turnaround (rather than virial) scale has many advantages: From a theoretical point of view, turnaround is a much better defined point in the spherical collapse model. Furthermore, non-sphericities are smaller at turnaround and that makes spherical collapse model more accurate when studying turnaround rather than virialized structures. Also, numerical simulations, theoretical and observational arguments show that no special physical meaning can be assigned to the the virial radius, as calculated through density-threshold arguments. Its not, for example, the boundary between a region of zero mean radial velocity with a region where material is in-falling or out-falling from the central region. On the other hand, turnaround is observationally defined as the non-expanding shell furthest away from the center of a bound structure. It separates the region where the gravitational attraction of the central structure is dominant, from the region where matter follows the general expansion of the Universe. In this sense, it is a very unambiguous boundary of a structure.

4.3 The Time Evolution of Turnaround Radius

We start by considering the evolution of the turnaround radius of a cosmic structure. Let $\delta_{\rm ta}(a)$ be the overdensity of a turnaround structure at cosmic epoch a, as obtained from the spherical collapse model (see also the following section). Then, from its definition:

$$\delta_{\rm ta}(a) \equiv \frac{\rho_{\rm ta}(a) - \rho_{\rm m}(a)}{\rho_{\rm m}(a)}, \tag{4.3.1}$$

where $\rho_{\rm ta}(a)$ is the density of the turnaround structure at turnaround and at cosmic epoch a, and $\rho_{\rm m}(a)$ is the mean matter density of the Universe at the same cosmic epoch. If we further assume that the turnaround structure is a sphere of constant density with total mass M, then:

$$\rho_{\rm ta}(a) = \frac{M}{\frac{4}{3}\pi R^3_{\rm ta}(a)} \tag{4.3.2}$$

with $R_{\rm ta}$ being the turnaround radius. From eqs. (4.3.1) and (4.3.2), and using that $\rho_{\rm m} = \rho_{\rm m,0}/a^3$, we get the turnaround radius as a function of cosmic epoch a:

$$R_{\rm ta}(a) = \left[\frac{3}{4\pi(1+\delta_{\rm ta}(a))\rho_{\rm m,0}}\right]^{1/3} a\ M^{1/3}, \tag{4.3.3}$$

with $\rho_{\rm m,0}$ the mean matter density of the Universe today.

In a recent work (See Tanoglidis, Pavlidou & Tomaras (2015)), we have shown that in ΛCDM a special mass scale exists, which separates structures with qualitatively different cosmological evolution. We have called this mass scale the *transitional* mass scale, which we have calculated to be:

$$M_{\rm transitional} \simeq 10^{13} M_{\odot}. \tag{4.3.4}$$

A convenient normalization of eq. (4.3.3) would be one that makes use of the importance of the transitional mass scale. For this reason, we define:

$$M^* \equiv 10^{13} M_{\odot}, \tag{4.3.5}$$

which is the order of magnitude of the transitional mass scale. We also define a related length scale, as the radius of the sphere which has mass M^* and density equal to the current critical density of the Universe, $\rho_{\rm c,0}$:

$$R^* \equiv \left(\frac{3M^*}{4\pi\rho_{\rm c,0}}\right)^{1/3} \cong 2.05\, h^{-2/3}\ {\rm Mpc}, \tag{4.3.6}$$

h being the dimensionless Hubble parameter. Expressing radii and masses in terms of R^* and M^*, respectively, eq. (4.3.3) becomes:

$$\frac{R_{\rm ta}(a)}{R^*} = \left[(1+\delta_{\rm ta}(a))\Omega_{\rm m,0}\right]^{-1/3} a \left(\frac{M}{M^*}\right)^{1/3}, \tag{4.3.7}$$

where $\Omega_{\rm m,0} \equiv \rho_{\rm m,0}/\rho_{\rm c,0}$.

We can isolate the part which gives the time evolution of the turnaround radius that does not depend on the mass of the structure, by taking logarithms on both parts of eq. (4.3.7):

$$\log\left(\frac{R_{\rm ta}(a)}{R^*}\right) = \frac{1}{3}\log\left(\frac{M}{M^*}\right) + \log\left(\left[(1+\delta_{\rm ta}(a))\Omega_{\rm m,0}\right]^{-1/3} a\right). \tag{4.3.8}$$

The mentioned time evolution has been isolated in the second logarithm of the R.H.S. of eq. (4.3.8). We define this part as:

$$I(a) \equiv \log\left(\left[(1+\delta_{\rm ta}(a))\Omega_{\rm m,0}\right]^{-1/3} a\right). \tag{4.3.9}$$

With this definition:

$$\log\left(\frac{R_{\rm ta}(a)}{R^*}\right) = I(a) + \frac{1}{3}\log\left(\frac{M}{M^*}\right). \tag{4.3.10}$$

For a theoretical calculation of $I(a)$ we need to know $\delta_{\rm ta}(a)$, i.e. how the turnaround overdensity evolves with time for different cosmologies. In the following subsection, we show how we can calculate this overdensity for different combinations of $\Omega_{\rm m,0}$ and $\Omega_{\Lambda,0}$, in the context of the simple spherical top-hat model.

4.4 Spherical Collapse Model

Here we will show how we can use the spherical collapse model in order to calculate the turnaround overdensity. The turnaround overdensity is given by:

$$\boxed{\delta_{\rm ta}(a) = \left(\frac{a}{a_{\rm p,ta}(a)}\right)^3 - 1,} \tag{4.4.1}$$

where $a_{\rm p,ta}(a)$ is the scale factor of a spherical perturbation/overdensity that turns around at time a, a being the scale factor of the Universe. Considering the perturbation as spherical, homogeneous and isotropic we can write a Friedmann equation for it. Using that, as well as the Friedmann equation for the background Universe, we can found how the perturbation evolves with scale factor, and then from (4.4.1) calculate the turnaround overdensity.

4.4.1 A Matter Dominated Universe

As a warm-up, we start from the case where the Universe contains only matter. The Friedmann equation for a perturbation in such a Universe can be written as:

$$\left(\frac{da_{\rm p}}{dt}\right)^2 = H_0^2\Omega_{\rm m,0}\left(a_{\rm p}^{-1} - \kappa\right), \tag{4.4.2}$$

where $\kappa > 0$ for an overdensity. Since $\frac{da_{\rm p}}{dt} = 0$ at turnaround, it follows immediately that:

$$\kappa = \frac{1}{a_{\rm p,ta}}, \tag{4.4.3}$$

which works for **any** positive κ. Now we want to get a similar equation for the background Universe. But we have to be very careful, so let us start from the Friedmann equation in the usual form (for the scale factor of the Universe) in a Universe only with matter:

$$\left(\frac{da}{dt}\right)^2 = \frac{8\pi G}{3}\rho_{\rm m,0}a^{-1} - \frac{kc^2}{R_0^2} \tag{4.4.4}$$

where R_0 is the curvature radius of the Universe. We can rewrite the above, using the definition of Hubble's constant, critical density and density parameter as:

$$\left(\frac{da}{dt}\right)^2 = H_0^2\Omega_{\rm m,0}\left(a^{-1} - \frac{kc^2}{R_0^2H_0^2\Omega_{\rm m,0}}\right). \tag{4.4.5}$$

It's really ugly, and it also depends on the curvature radius, a not "known" cosmological parameter. But, the Friedmann equation can also be written as:

$$H^2 = H^2\Omega_{\rm m} - \frac{kc^2}{R_0^2a^2} \tag{4.4.6}$$

so, solving for the present time ($a = 1$) we have that:

$$\frac{kc^2}{R_0} = H_0^2\left(\Omega_{\rm m,0} - 1\right). \tag{4.4.7}$$

Then, substituting (4.4.7) to (4.4.5), we get:

$$\left(\frac{da}{dt}\right)^2 = H_0^2 \Omega_{\mathrm{m},0} \left(a^{-1} + \frac{1-\Omega_{\mathrm{m},0}}{\Omega_{\mathrm{m},0}}\right). \tag{4.4.8}$$

To find the behaviour of the the perturbation radius as a function of the scale factor of the Universe, we divide (4.4.2) with (4.4.8). We get:

$$\left(\frac{da_{\mathrm{p}}}{da}\right)^2 = \frac{a}{a_{\mathrm{p}}} \frac{1-\kappa a_{\mathrm{p}}}{1+\left(\frac{1-\Omega_{\mathrm{m},0}}{\Omega_{\mathrm{m},0}}\right) a}. \tag{4.4.9}$$

Now, we set $\kappa = a_{\mathrm{p,ta}}^{-1}$, and also we get the positive square root:

$$\frac{da_{\mathrm{p}}}{da} = \frac{\sqrt{a}}{\sqrt{a_{\mathrm{p}}}} \frac{\sqrt{1-a_{\mathrm{p,ta}}^{-1} a_{\mathrm{p}}}}{\sqrt{1+\left(\frac{1-\Omega_{\mathrm{m},0}}{\Omega_{\mathrm{m},0}}\right) a}}. \tag{4.4.10}$$

Then, separating variables and integrating, we get:

$$\int_0^{a_{\mathrm{p}}} \frac{\sqrt{y}}{\sqrt{1-a_{\mathrm{p,ta}}^{-1} y}} \quad dy = \int_0^{a} \frac{\sqrt{x}}{\sqrt{1+\left(\frac{1-\Omega_{\mathrm{m},0}}{\Omega_{\mathrm{m},0}}\right) x}} \quad dx \tag{4.4.11}$$

Now, let us treat R.H.S integral. We make a change of variables $u = \frac{y}{a_{\mathrm{p,ta}}} \Rightarrow y = u a_{\mathrm{p,ta}}$. Defining $r \equiv \frac{a_{\mathrm{p}}}{a_{\mathrm{p,ta}}}$, which is the upper limit when we change variables, we get that the R.H.S. integral is equal to:

$$a_{\mathrm{p,ta}}^{3/2} \int_0^{r} \frac{\sqrt{u}}{\sqrt{1-u}} \quad du \tag{4.4.12}$$

Eq. (4.4.11) becomes:

$$a_{\mathrm{p,ta}}^{3/2} \int_0^{r} \frac{\sqrt{u}}{\sqrt{1-u}} \quad du = \int_0^{a} \frac{\sqrt{x}}{\sqrt{1+\left(\frac{1-\Omega_{\mathrm{m},0}}{\Omega_{\mathrm{m},0}}\right) x}} \quad dx. \tag{4.4.13}$$

When $a_{\mathrm{p}} = a_{\mathrm{p,ta}} \Rightarrow r = 1$ and then $a = a_{\mathrm{ta}}$. But for upper limit $r = 1$ we have:

$$\int_0^{1} \frac{\sqrt{u}}{\sqrt{1-u}} \quad du = \frac{\pi}{2}. \tag{4.4.14}$$

Then, we finally get our answer:

$$a_{\mathrm{p,ta}} = \left[\frac{2}{\pi} \int_0^{a_{\mathrm{ta}}} \frac{\sqrt{x}}{\sqrt{1+\left(\frac{1-\Omega_{\mathrm{m},0}}{\Omega_{\mathrm{m},0}}\right) x}} \quad dx\right]^{2/3}. \tag{4.4.15}$$

When $\Omega_{\mathrm{m},0} = 1$, the integral has analytic solution:

$$\int_0^{a_{\mathrm{ta}}} \frac{\sqrt{x}}{\sqrt{1+0\cdot x}} \quad dx = \int_0^{a_{\mathrm{ta}}} \sqrt{x} \quad dx = \frac{2}{3} a_{\mathrm{ta}}^{3/2}. \tag{4.4.16}$$

So we get that:

$$\left(\frac{a_{\rm ta}}{a_{\rm p,ta}}\right)^3 = \left(\frac{3}{4}\pi\right)^2 \cong 5.55. \tag{4.4.17}$$

From eq. (4.4.1) we then have:

$$\delta_{\rm ta} \cong 4.55, \tag{4.4.18}$$

which is the well-known result in the literature for a flat, matter-dominated Universe. Note that this is constant, independent of time. For all other cosmologies the result depends on time.

4.4.2 ΛCDM Cosmology

Let us generalize now, considering a perturbation in a Universe (flat, open or closed) with matter AND a cosmological constant. The evolution of perturbation in a Universe with matter and Lambda is dictated now by the equation:

$$\left(\frac{da_{\rm p}}{dt}\right)^2 = H_0^2\Omega_{\rm m,0}\frac{1}{a_{\rm p}}\left(\omega a_{\rm p}^3 - \kappa a_{\rm p} + 1\right), \tag{4.4.19}$$

where we have defined:

$$\omega \equiv \frac{\Omega_{\Lambda,0}}{\Omega_{\rm m,0}}. \tag{4.4.20}$$

From eq. (4.4.19), it is clear that (since the derivative is zero at turnaround):

$$\kappa = \frac{\omega a_{\rm p,ta}^3 + 1}{a_{\rm p,ta}} \tag{4.4.21}$$

For the background Universe, working as in the previous section, and noting that here:

$$\frac{kc^2}{R_0^2} = H_0^2\left(\Omega_{\rm m,0} + \Omega_{\Lambda,0} - 1\right), \tag{4.4.22}$$

we have:

$$\left(\frac{da}{dt}\right)^2 = H_0^2\Omega_{\rm m,0}\frac{1}{a}\left(\omega a^3 + \xi a + 1\right). \tag{4.4.23}$$

In the previous equation we have also defined:

$$\xi \equiv \frac{1 - \Omega_{\rm m,0} - \Omega_{\Lambda,0}}{\Omega_{\rm m,0}} \tag{4.4.24}$$

Dividing now eqs. (4.4.19) with (4.4.23), we get:

$$\left(\frac{da_{\rm p}}{da}\right)^2 = \frac{a}{a_{\rm p}}\frac{\omega a_{\rm p}^3 - \kappa a_{\rm p} + 1}{\omega a^3 + \xi a + 1}. \tag{4.4.25}$$

Taking square roots in both sides, separating variables and integrating we get:

$$\underbrace{\int_0^{a_{\rm p}} \frac{\sqrt{y}}{\sqrt{\omega y^3 - \kappa y + 1}}\ dy}_{I} = \int_0^a \frac{\sqrt{x}}{\sqrt{\omega x^3 + \xi x + 1}}\ dx. \tag{4.4.26}$$

Let us treat now the L.H.S integral. At first, we perform a change of variables $u = \frac{y}{a_{\rm p,ta}}$, $r = \frac{a_{\rm p}}{a_{\rm p,ta}}$ as before. The integral becomes:

$$I = {a_{\rm p,ta}}^{3/2} \int_0^r \frac{\sqrt{u}}{\sqrt{\omega u^3 {a_{\rm p,ta}}^3 - \kappa a_{\rm p,ta} u + 1}} \quad du. \tag{4.4.27}$$

Substituting κ from (4.4.21), we get:

$$I = {a_{\rm p,ta}}^{3/2} \int_0^r \frac{\sqrt{u}}{\sqrt{\omega u^3 {a_{\rm p,ta}}^3 - \left(\frac{\omega a_{\rm p,ta}^3 + 1}{a_{\rm p,ta}}\right) a_{\rm p,ta} u + 1}} \quad du \Rightarrow \qquad (\text{for } \omega \neq 0)$$

$$\Rightarrow I = {a_{\rm p,ta}}^{3/2} \int_0^r \frac{\sqrt{u}}{\sqrt{\omega {a_{\rm p,ta}}^3 \left(u^3 - u + \frac{1-u}{\omega a_{\rm p,ta}^3}\right)}} \quad du \Rightarrow$$

$$\Rightarrow I = \frac{1}{\omega^{1/2}} \int_0^r \frac{\sqrt{u}}{\sqrt{(1-u)\left[\mu - u(u+1)\right]}} \quad du, \tag{4.4.28}$$

with:

$$\mu \equiv \frac{1}{\omega a_{\rm p,ta}^3} \tag{4.4.29}$$

Then eq. (4.4.26) becomes:

$$\frac{1}{\omega^{1/2}} \int_0^r \frac{\sqrt{u}}{\sqrt{(1-u)\left[\mu - u(u+1)\right]}} \quad du = \int_0^a \frac{\sqrt{x}}{\sqrt{\omega x^3 + \xi x + 1}} \quad dx. \tag{4.4.30}$$

For turnaround we have, by definition, $r = 1, \mu = \mu_{\rm ta}, a = a_{\rm ta}$, so:

$$\int_0^1 \frac{\sqrt{u}}{\sqrt{(1-u)\left[\mu_{\rm ta} - u(u+1)\right]}} \quad du = \omega^{1/2} \int_0^{a_{\rm ta}} \frac{\sqrt{x}}{\sqrt{\omega x^3 + \xi x + 1}} \quad dx. \tag{4.4.31}$$

This equation has to be solved numerically (the simplest method is the method of bisection) to give us $\mu_{\rm ta}$ and thus $a_{\rm p,ta}$ for every cosmic epoch $a_{\rm ta}$. In principle we can do it for every mixture of matter and cosmological constant densities we want.

Note: The L.H.S integral as presented in eq. (4.4.31) presents problems when we try to calcuate it numerically (e.g. with Simpson method). When $r = 1$ the integrand diverges. There is no way to heal this problem with e.g. careful take of limits or something else. Back to scratch-paper. We will do a nice change of variables inspired from the method we use to solve the integral:

$$\int_0^1 \frac{\sqrt{x}}{\sqrt{1-x}} \quad dx$$

We change variables:

$$u = \sin^2\theta, \quad du = 2\sin\theta\cos\theta d\theta, \quad \text{upper limit} = \pi/2, \quad \text{lower limit} = 0, \tag{4.4.32}$$

and eq. (4.4.31) becomes:

$$\int_0^{\pi/2} \frac{\sin^2\theta}{\sqrt{\mu_{\rm ta} - \sin^2\theta\left(\sin^2\theta + 1\right)}} \quad d\theta = \frac{\omega^{1/2}}{2} \int_0^{a_{\rm ta}} \frac{\sqrt{x}}{\sqrt{\omega x^3 + \xi x + 1}} \quad dx. \tag{4.4.33}$$

The integrand now has no problem at the limits, so we can use the usual numerical integration methods.

As a last word, let us say a few words about the maximum turnaround radius in the ΛCDM model. Consider again equation (4.4.21):

$$\kappa = \frac{\omega a_{\rm p,ta}^3 + 1}{a_{\rm p,ta}}.$$

The parameter κ (> 0 for an overdensity) characterises the magnitude of the perturbation. There is a minimum κ such that the perturbation to be able to turnaround, i.e. to satisfy the above equation. Cosnisder κ as a function of the turnaround radius, $a_{\rm p,ta}$. We find the the $a_{\rm p,ta}$ which minimizes it, by setting $d\kappa/da_{\rm p,ta} = 0$. This gives the minimum value of κ for turnaround and collapse, and the corresponding maximum value of the turnaround radius:

$$k_{\rm min,coll} = \frac{3\omega^{1/3}}{2^{2/3}}, \qquad a_{\rm p,ta,max} = (2\omega)^{1/3}. \tag{4.4.34}$$

The physical radius of a perturbation with scale factor $a_{\rm p}$ is $R_{\rm p} = a_{\rm p}\left(\frac{3M}{4\pi\rho_{\rm p}}\right)^{1/3}$. With this, the result of equation (4.4.34) coincides with that of eq. (4.1.1).

4.4.3 Clustering Dark Energy

Consider now a Universe with matter and an element with density that scales as:

$$\rho \propto \frac{1}{a^{3(1+w)}}, \tag{4.4.35}$$

for the background Universe and:

$$\rho \propto \frac{1}{a_{\rm p}^{3(1+w)}}, \tag{4.4.36}$$

for a perturbation in this Universe. w is the equation of state parameter of that element. If $w < -1/3$ the element is characterized as **dark energy**. Especially, if $w < -1$ it is characterized as **phantom energy**. For the case where this element follows the evolution of a perturbation (is not homogeneous, doesn't scale with the background Universe even we consider a perturbation) is called **clustering** dark energy.

Analogously with eq. (4.4.19) we have now the equation that describes a perturbation in such a Universe:

$$\left(\frac{da_{\rm p}}{dt}\right)^2 = H_0^2\Omega_{\rm m,0}\frac{1}{a_{\rm p}}\left(\omega a_{\rm p}^{-3w} - \kappa a_{\rm p} + 1\right), \tag{4.4.37}$$

with ω now defined as:

$$\omega \equiv \frac{\Omega_{\rm de,0}}{\Omega_{\rm m,0}}, \tag{4.4.38}$$

where $\Omega_{\rm de,0}$ denoting the current **dark energy density**. From eq. (4.4.37) we have at turnaround ($da_p/dt = 0$):

$$\omega a_{\rm p,ta}^{-3w} - \kappa a_{\rm p,ta} + 1 = 0 \Rightarrow$$

$$\Rightarrow \kappa = \frac{\omega a_{\rm p,ta}^{-3w} + 1}{a_{\rm p,ta}}. \tag{4.4.39}$$

Similarly, for the background Universe we have:

$$\left(\frac{da}{dt}\right)^2 = H_0^2 \Omega_{\rm m,0} \frac{1}{a} \left(\omega a^{-3w} + \xi a + 1\right), \tag{4.4.40}$$

with:

$$\xi \equiv \frac{1 - \Omega_{\rm m,0} - \Omega_{\rm de,0}}{\Omega_{\rm m,0}}. \tag{4.4.41}$$

Dividing equations (4.4.37) and (4.4.40), we have:

$$\left(\frac{da_{\rm p}}{da}\right)^2 = \frac{a}{a_{\rm p}} \frac{\omega a_{\rm p}^{-3w} - \kappa a_{\rm p} + 1}{\omega a^{-3w} + \xi a + 1}. \tag{4.4.42}$$

Separating variables and integrating, we get:

$$\underbrace{\int_0^{a_{\rm p}} \frac{\sqrt{y}}{\sqrt{\omega y^{-3w} - \kappa y + 1}} \, dy}_{I} = \int_0^{a} \frac{\sqrt{x}}{\sqrt{\omega x^{-3w} + \xi x + 1}} \, dx \tag{4.4.43}$$

Again, let us treat L.H.S integral, I. Performing a change of variables $u = \frac{y}{a_{\rm p,ta}}$, $r = \frac{a_{\rm p}}{a_{\rm p,ta}}$, the integral becomes:

$$I = {a_{\rm p,ta}}^{3/2} \int_0^{r} \frac{\sqrt{u}}{\sqrt{\omega u^{-3w} {a_{\rm p,ta}}^{-3w} - \kappa a_{\rm p,ta} u + 1}} \, du \tag{4.4.44}$$

Substituting κ from (4.4.39) we have:

$$I = {a_{\rm p,ta}}^{3/2} \int_0^{r} \frac{\sqrt{u}}{\sqrt{\omega u^{-3w} {a_{\rm p,ta}}^{-3w} - \frac{\omega a_{\rm p,ta}^{-3w} + 1}{a_{\rm p,ta}} a_{\rm p,ta} u + 1}} \, du \Rightarrow \tag{4.4.45}$$

$$\Rightarrow I = {a_{\rm p,ta}}^{3/2} \int_0^{r} \frac{\sqrt{u}}{\sqrt{\omega u^{-3w} {a_{\rm p,ta}}^{-3w} - u\omega a_{\rm p,ta}^{-3w} - u + 1}} \, du \Rightarrow \tag{4.4.46}$$

$$\Rightarrow I = {a_{\rm p,ta}}^{3/2} \int_0^{r} \frac{\sqrt{u}}{\sqrt{\omega {a_{\rm p,ta}}^{-3w} (u^{-3w} - u) + 1 - u}} \, du. \tag{4.4.47}$$

Equating this with R.H.S of (4.4.43) (with $r = 1$ at turnaround), we find the scale factor of the perturbation at turnaround as a function of the scale factor of the Universe:

$$I = {a_{\rm p,ta}}^{3/2} \int_0^{1} \frac{\sqrt{u}}{\sqrt{\omega {a_{\rm p,ta}}^{-3w} (u^{-3w} - u) + 1 - u}} \, du = \int_0^{a_{\rm ta}} \frac{\sqrt{x}}{\sqrt{\omega x^{-3w} + \xi x + 1}} \, dx \tag{4.4.48}$$

Unfortunately, we cannot simplify further this complicated equation and it has to be solved numerically, in order to find $a_{\rm p,ta}$ for any $a_{\rm ta}$.

Now let's investigate which is the maximum turnaround radius when considering a general, constant-w, clustering dark energy cosmology. We will start from equation (4.4.37):

$$\left(\frac{da_{\rm p}}{dt}\right)^2 = H_0^2\Omega_{\rm m,0}\frac{1}{a_{\rm p}}\left(\omega a_{\rm p}^{-3w} - \kappa a_{\rm p} + 1\right).$$

And we are searching for the minimum κ such that the perturbation to be able to have turnaround, i.e.:

$$\omega a_{\rm p,tu}^{-3w} - \kappa a_{\rm p,ta} + 1 = 0 \Rightarrow \kappa = \omega a_{\rm p,ta}^{-(1+3w)} + \frac{1}{a_{\rm p,ta}} \tag{4.4.49}$$

We treat κ as a function of the turnaround radius, i.e. $\kappa \equiv \kappa\left(a_{\rm p,ta}\right)$. In order to minimize κ set it's derivative with respect to $a_{\rm p,ta}$ equal to zero:

$$\frac{\partial\kappa(a_{\rm p,tu})}{\partial a_{\rm p,tu}} = 0 \quad \Rightarrow \quad -(1+3w)\ \omega\ a_{\rm p,ta}^{-(2+3w)} - \frac{1}{a_{\rm p,ta}} = 0. \tag{4.4.50}$$

In order this equation to be able to be satisfied we must have (since $a_{\rm p,ta},\ \omega$ are positive quantities):

$$-(1+3w) > 0 \Rightarrow 1+3w < 0 \Rightarrow w < -\frac{1}{3}, \tag{4.4.51}$$

which is the condition for the dark energy, and this shows that every dark energy component causes a maximum turnaround radius to exist. Now, having in mind this condition, we find the $a_{\rm p,ta}$ which minimizes κ to be (from (4.4.50)):

$$-(1+3w)\ \omega\ a_{\rm p,ta}^{-(2+3w)} - \frac{1}{a_{\rm p,ta,max}} = 0 \Rightarrow -(1+3w)\omega = a_{\rm p,ta,max}^{-2} a_{\rm p,ta,max}^{2+3w} \Rightarrow \tag{4.4.52}$$

$$\boxed{a_{\rm p,ta,max} = \left[-(1+3w)\ \omega\right]^{\frac{1}{3w}}.} \tag{4.4.53}$$

For $w = -1$ (cosmological constant), this gives:

$$a_{\rm p,ta,max} = (2\omega)^{-1/3}, \tag{4.4.54}$$

which is the well-known result (see previous subsection). The minimum κ correspondingly is:

$$\kappa_{\rm min,coll} = \omega[-(1+3w)\omega]^{-\frac{1+3w}{3w}} + [-(1+3w)\omega]^{-\frac{1}{3w}} \Rightarrow \tag{4.4.55}$$

$$\kappa_{\rm min,coll} = \frac{3w}{1+3w}\left[-(1+3w)\omega\ \right]^{-\frac{1}{3w}}. \tag{4.4.56}$$

For $w = -1$ this gives:

$$\kappa_{\rm min,coll} = \frac{3}{2^{2/3}}\omega^{1/3}, \tag{4.4.57}$$

which also agrees with the known result.

4.4.4 Homogeneous Dark Energy

Consider now an energy component which scales as:

$$\rho_{\rm de} \propto \frac{1}{a^{3(1+w)}}, \qquad (w < -1/3) \tag{4.4.58}$$

even we are considering an overdensity (i.e. it always scales with the scale factor of the background Universe. In this case we have a **homogeneous** dark energy. We make the following definitions:

$$\omega \equiv \frac{\Omega_{\rm de,0}}{\Omega_{\rm m,0}}, \qquad \xi \equiv \frac{1-\Omega_{\rm m,0}-\Omega_{\rm de,0}}{\Omega_{\rm m,0}}. \tag{4.4.59}$$

The equation which describes the evolution of a matter perturbation in a Universe with homogeneous dark energy and matter is:

$$\left(\frac{da_{\rm p}}{dt}\right)^2 = H_0^2\Omega_{\rm m,0}\frac{1}{a_{\rm p}}\left(\omega a_{\rm p}^3 a^{-3(1+w)} - \kappa a_{\rm p} + 1\right). \tag{4.4.60}$$

While, for the evolution of the background Universe we have the equation:

$$\left(\frac{da}{dt}\right)^2 = H_0^2\Omega_{\rm m,0}\frac{1}{a}\left(\omega a^{-3w} + \xi a + 1\right). \tag{4.4.61}$$

Dividing eqs. (4.4.60) and (4.4.61) we get:

$$\left(\frac{da_{\rm p}}{da}\right)^2 = \frac{a}{a_{\rm p}}\frac{\omega a_{\rm p}^3 a^{-3(1+w)} - \kappa a_{\rm p} + 1}{\omega a^{-3w} + \xi a + 1}. \tag{4.4.62}$$

Solving this we can in principle determine the evolution of a perturbation in terms of the scale factor of the Universe. Again, κ is a parameter related to the size and sign of the perturbation. Since $\frac{da_{\rm p}}{da} = 0$ at turnaround, we can write:

$$\kappa = \frac{\omega a_{\rm p,ta}^3 a_{\rm ta}^{-3(1+w)} + 1}{a_{\rm p,ta}}. \tag{4.4.63}$$

Treating $a_{\rm ta}$ as a fixed parameter, we get the $a_{\rm p,ta}$ which gives the minimum κ for turnaround. That is:

$$a_{\rm p,ta,max} = a_{\rm ta}^{1+w}\left[2\omega\right]^{-1/3} \tag{4.4.64}$$

and corresponding minimum κ is:

$$\kappa_{\rm min,\ coll} = a_{\rm ta}^{-(1+w)}\frac{3\omega^{1/3}}{2^{2/3}} \tag{4.4.65}$$

Expressions (4.4.64) and (4.4.65) have meaning only in the case $a_{\rm ta} \to \infty$. Which means:

$$a_{\rm p,ta,max} = \begin{cases} \infty, & w > -1 \\ \left[2\omega\right]^{-1/3}, & w = -1 \\ 0, & w < -1 \end{cases} \tag{4.4.66}$$

and

$$\kappa_{\rm min,coll} = \begin{cases} 0, & w > -1 \\ \frac{3\omega^{1/3}}{2^{2/3}}, & w = -1 \\ \infty, & w < -1 \end{cases} \tag{4.4.67}$$

Ok, now our aim is to find the evolution of $a_{\rm p,ta}$ (not $a_{\rm p,ta,max}$) as a function of a. I will make the following change of variables in eq. (4.4.62):

$$x \equiv \frac{a}{a_{\rm ta}}, \qquad \Rightarrow \qquad a = a_{\rm ta}\, x \tag{4.4.68}$$

$$y \equiv \frac{a_{\rm p}}{a_{\rm p,ta}} \qquad \Rightarrow \qquad a_{\rm p} = a_{\rm p,ta}\, y \tag{4.4.69}$$

Changing variables this way and also substituting κ from the expression in (6), we get:

$$\left(\frac{dy}{dx}\right)^2 = \frac{a_{\rm ta}^3}{a_{\rm p,ta}^3}\frac{x}{y}\frac{\omega a_{\rm p,ta}^3 a_{\rm ta}^{-3(1+w)} y\left(y^2 x^{-3(1+w)} - 1\right) + 1 - y}{\omega a_{\rm ta}^{-3w} x^{-3w} + \xi a_{\rm ta} x + 1} \tag{4.4.70}$$

Although this seems complicated, it has some merits. A perturbation which turnarounds at an epoch $a_{\rm ta}$ has $a_{\rm p,ta}$ such that $y = 1$ when $x = 1$. The differential equation has to be solved using standard numerical techniques.

Chapter 5

Probing Dark Energy at Turnaround II: Numerical Results

In the previous chapter, we reduced the problem of describing the time evolution of the turnaround radius of cosmic structures to the calculation of the function $I(a)$, eq. (4.3.9). The exact form of this function depends on cosmology explicitly through the value of $\Omega_{\rm m,0}$ and also through the turnaround overdensity, $\delta_{\rm ta}(a)$, which is different for different combinations of the cosmological parameters ($\Omega_{\rm m,0}$ and $\Omega_{\Lambda,0}$ in the ΛCDM model and also on the equation of state parameter, w, in general dark energy models). We also showed how to use the spherical collapse model in order to calculate the turnaround overdensity for a general combination of these parameters.

In this chapter, we use these results to demonstrate how the values of the present matter and cosmological constant density parameters, as well as of the equation of state parameter, are imprinted in the evolution history of the turnaround radius. For this reason we plot the theoretical predictions for $I(a)$ for different cosmologies. The results presented here show that the existence of a cosmological constant in the Universe has a profound local effect that –in principle– can be measured. Then, we propose a way for a local measurement of the cosmological constant density. We also show the dependence on w, for constant matter and dark energy density parameters, for clustering and homogeneous dark energy.

5.1 ΛCDM Cosmology

5.1.1 Constant matter density

We start by considering models with different values for the cosmological constant energy density, $\Omega_{\Lambda,0}$, but with the same value for the matter density, $\Omega_{\rm m,0} = 0.30$ (roughly the currently accepted value). For the $\Omega_{\Lambda,0}$ we have chosen values in the range $[0.00, 1.50]$. Our aim is to show that, following the evolution of turnaround radii of structures, we are in principle able to distinguish between different values of $\Omega_{\Lambda,0}$; especially between models with and without a cosmological constant.

In figure 5.1 we plot $I(a)$, eq. (4.3.9), as a function of a, from $a \sim 0$ to $a = 2.00$ and for the values of cosmological parameters mentioned above. In an inset figure, we present $I(a)$ for the same sets of parameters, but in a narrower range in a, around the point where all graphs of the bigger plot seem to intersect. From this

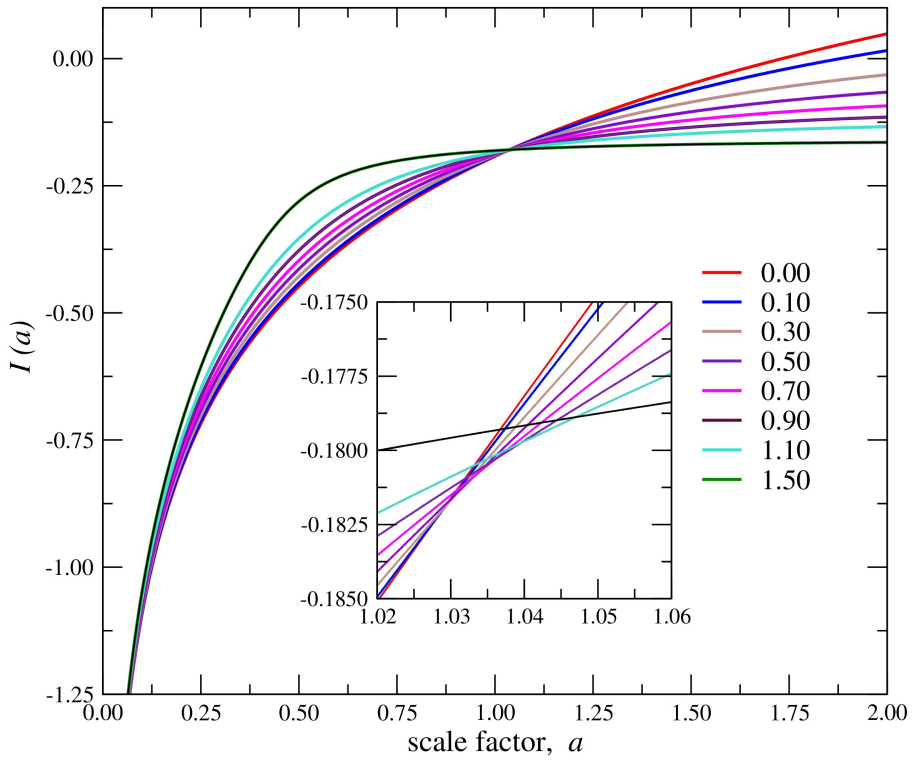

Figure 5.1: $I(a)$ as a function of a, for constant $\Omega_{\mathrm{m},0} = 0.30$, and different values of $\Omega_{\Lambda,0}$, in a range from $\Omega_{\Lambda,0} = 0.00$ to $\Omega_{\Lambda,0} = 1.50$. The inset figure presents $I(a)$ for the same parameters as in the greater figure, but in a shorter range in a, around the point where all graphs seem to intersect in the greater figure.

figure we can see how different values of $\Omega_{\Lambda,0}$ predict different evolution histories, $I(a)$. Let us discuss the main features of this plot.

From the plot it can be inferred that for models with high value for $\Omega_{\Lambda,0}$, $I(a)$ approaches a constant value. Indeed, as we discuss below, this is also true for any model with a non-zero cosmological constant, even it is not clear in this plot, since in models with a smaller value for $\Omega_{\Lambda,0}$, $I(a)$ approaches its ultimate value later. Also, we can see that ultimate value of $I(a)$, $I_{\mathrm{ult}} = I(a \to \infty)$, is smaller, the higher the value of $\Omega_{\Lambda,0}$ is. This behaviour can easily be explained, using eq. 4.1.1 for the ultimate / maximum value for the turnaround radius. Expressing and masses and radii in terms of M^* and R^*, (eqs. (4.3.5) and (4.3.6)), and taking logarithms in both sides, we get:

$$\log\left(\frac{R_{\mathrm{ta,max}}}{R^*}\right) = \frac{1}{3}\log\left(\frac{4\pi G\rho_{\mathrm{c},0}}{\Lambda c^2}\right) + \frac{1}{3}\log\left(\frac{M}{M^*}\right), \tag{5.1.1}$$

where we have used the definition of R^*, eq. (4.3.6). Comparing this with eq. (4.3.10), we see that:

$$I_{\mathrm{ult}} = \frac{1}{3}\log\left(\frac{4\pi G\rho_{\mathrm{c},0}}{\Lambda c^2}\right) = \frac{1}{3}\log\left(\frac{4\pi G\rho_{\mathrm{c},0}}{c^2}\right) - \frac{1}{3}\log\Lambda. \tag{5.1.2}$$

As it is clear from the above equation, $I(a)$ approaches a constant value which is lower for a higher value of Λ, exactly as it can be inferred from the plot.

An interesting feature of the plot is that at the present epoch ($a = 1.00$) I has almost the same value for all models (for all values of $\Omega_{\Lambda,0}$). Additionally, I seems to have exactly the same value (the graphs intersect) for every value of $\Omega_{\Lambda,0}$ a little later, at an point, let us call it a_{int}. The inset picture, which focuses around that point, demonstrates that indeed, this is not unique for all graphs. The intersection point a pair of graphs is a little bit different from that of another pair of graphs. However, all are very close, compared to the range where we plot I in the greater figure. For this reason, in the analysis which follows, we thing of an effectively unique point of intersection a_{int} around $a \sim 1.03 - 1.04$ for all graphs. Then we can see that for $a < a_{int}$ we have $I_1(a) > I_2(a)$ if $(\Omega_{\Lambda,0})_1 > (\Omega_{\Lambda,0})_2$, while for $a > a_{int}$ we have $I_1(a) < I_2(a)$ if $(\Omega_{\Lambda,0})_1 > (\Omega_{\Lambda,0})_2$.

We can understand qualitatively the above behaviour: Consider two models with the same $\Omega_{\rm m,0}$ and $(\Omega_{\Lambda,0})_1 > (\Omega_{\Lambda,0})_2$. A larger value of the cosmological constant in the first model implies that, in order for the two models to end up with the same matter density today, in the past the first model had to have (much) larger matter density than the second: $(\Omega_{\rm m,past})_1 > (\Omega_{\rm m,past})_2$, always. In a particular epoch, the dependence of the turnaround overdensity on the value of Ω_Λ is much weaker than the dependence on the value of $\Omega_{\rm m}$. And the higher the value of $\Omega_{\rm m}$ is, the lower is the value of the turnaround overdensity (it is "easier" for a structure to turn around). Thus $(\Omega_{\rm m,past})_1 > (\Omega_{\rm m,past})_2 \Rightarrow (\delta_{\rm ta,past})_1 < (\delta_{\rm ta,past})_2$. Then, from the definition of $I(a)$, eq. (4.3.9), $I(a) = \log a - (1/3)\log[(1 + \delta_{\rm ta}(a))\Omega_{\rm m,0}]$, a larger value of $\delta_{\rm ta}$ leads to a lower (more negative) value for I. Thus, the two models with $(\Omega_{\Lambda,0})_1 > (\Omega_{\Lambda,0})_2$ had in the past $I_1(a, past) > I_2(a, past)$.

Today, we also have $I_1 > I_2$, since for all the time in the past the first model had higher matter density and thus it was easier for turnaround to happen and this continues until today, where the two matter densities are the same. But in the future, the model which has higher Λ density today will have lower matter density, and thus then the turnaround overdensity will be higher. So, in the future: $I_1(a, future) < I_2(a, future)$, with ultimate values those predicted by (5.1.2). Since $I_1(a = 1) >= I_2(a = 1)$ (they have almost the same value), the point where the two graphs (for $I_1(a)$ and $I_2(a)$) intersect, a_{int} will be very close to the present epoch. Of course, the present is not special. Rather, it seems to be special because we demand $(\Omega_m)_1$ for all models to be identical today. Since, not only two, but all models, have similar values for I today and rapidly diverge and spread in the past and in the future, the point of intersection will be almost the same for all graphs, exactly as the plots presented here demonstrate.

5.1.2 Constant Λ density

It is also interesting to examine the evolution of $I(a)$ for models with constant $\Omega_{\Lambda,0}$ and different values for the current matter density, $\Omega_{\rm m,0}$. We chose $\Omega_{\Lambda,0} = 0.70$, close to the value that is inferred from non-local methods and $\Omega_{\rm m,0}$ in the range $[0.10, 0.60]$. In figure 5.2 we present $I(a)$ as a function of a, for $a \sim 0$ to $a = 2.00$ and for the values of cosmological parameters mentioned above.

In figure 5.2 we see that for all models, $I(a)$ reaches the *same* ultimate value. This behaviour can be directly explained referring to eq. (5.1.2): since all models have the same Λ density, they will all reach the same ultimate value, $I_{\rm ult}$, independently from the value of the current matter density of the Universe.

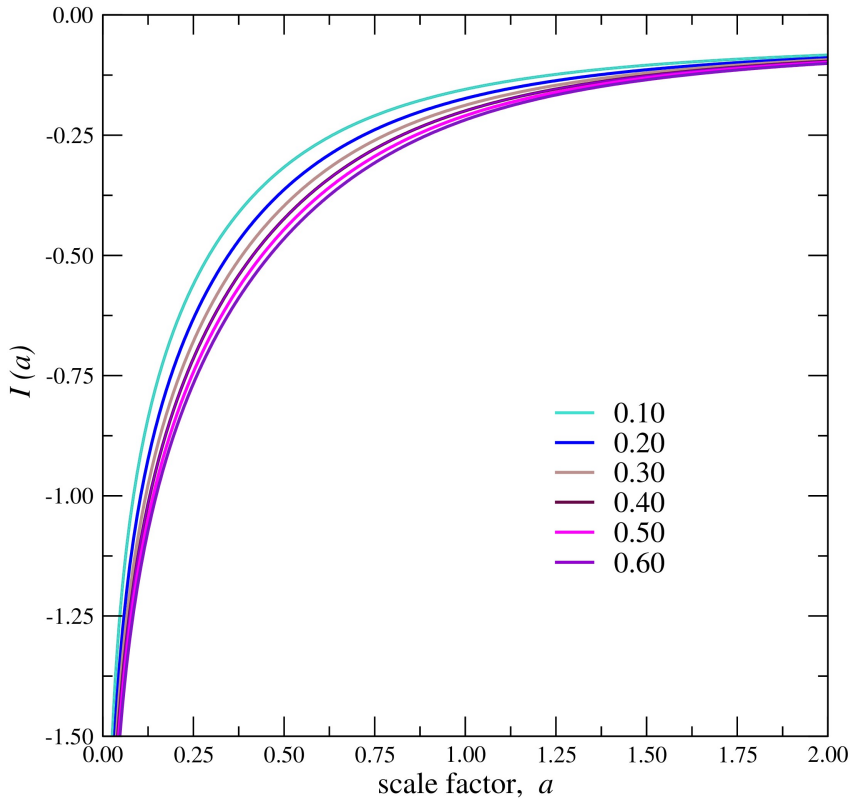

Figure 5.2: $I(a)$ as a function of a, for constant $\Omega_{\Lambda,0} = 0.70$, and different values of $\Omega_{\mathrm{m},0}$, in a range from $\Omega_{\mathrm{m},0} = 0.10$ to $\Omega_{\mathrm{m},0} = 0.60$.

We see that for two models, with $(\Omega_{\mathrm{m},0})_1 > (\Omega_{\mathrm{m},0})_2$ then $I_1(a) < I_2(a)$ *always*. Since all models have the same Λ density, if one model has greater matter density today than the other, it always had and it will always have greater matter density. The turnaround overdensity for the two models is $(\delta_{\mathrm{ta}})_1 < (\delta_{\mathrm{ta}})_2$. But from the definition of $I(a)$: $I(a) = \log\left([(1+\delta_{\mathrm{ta}}(a))\Omega_{\mathrm{m},0}]^{-1/3}\, a\right)$, at a particular epoch the dependence on $\Omega_{\mathrm{m},0}$ prevails, thus models with higher matter density give lower values for I.

5.1.3 Using turnaround for a *local* measurement of Λ density

What do we mean by the term *local*?

As we have stated in the introduction, our aim is to find a way to measure locally the value of the cosmological constant. Before presenting how this idea can be implemented using the results presented in the previous sections, it is necessary to clarify our use of the term *local*, to avoid misconceptions.

By the term local, we do not refer to the local universe. What we mean is that each measurement that goes into the method is itself local, i.e. does not depend on what the Universe is doing as a whole (for example, that its expansion is accelerating). It uses an effect of the cosmological constant in relatively short scales – the scales of the turnaround radii of cosmic structures.

Despite of this, our method still has to use data from the high-z universe. We have to look as far as distant supernovae searches look to find hints of dark energy.

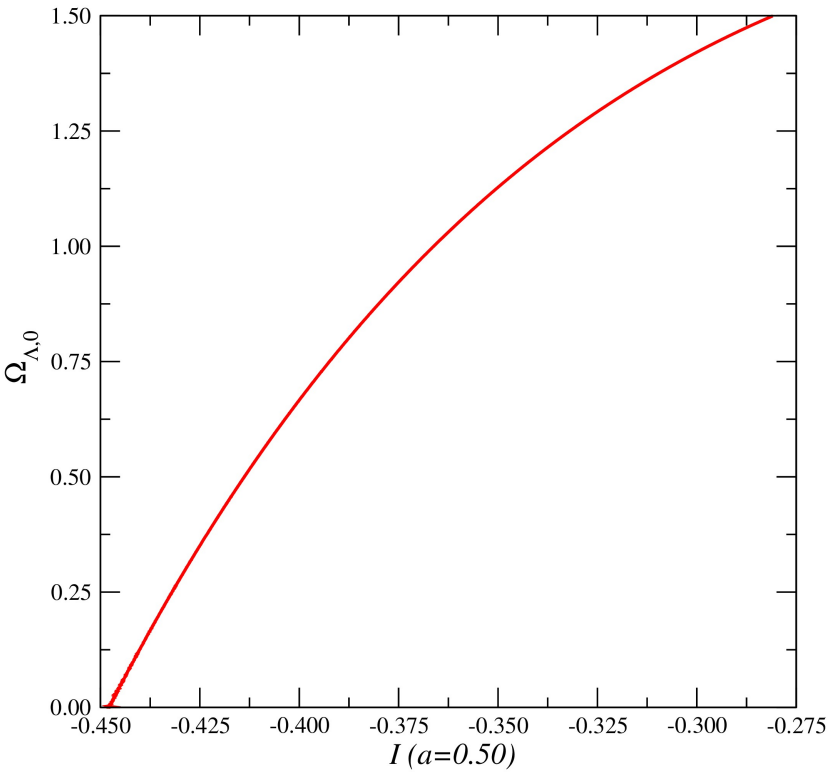

Figure 5.3: $\Omega_{\Lambda,0}$ as a function of I, at $a = 0.50$ and $\Omega_{\mathrm{m},0} = 0.30$, constant.

This is clear from the results presented in the previous section, where it can be seen that we have to look in the past in order to distinguish between models with the same matter density but different cosmological constant densities (optimally at $a \sim 0.50$, where the difference in the value of I for different models becomes maximum).

A worked example: towards a local proof that $\Lambda \neq 0$

Suppose that we are able to measure turnaround radii, R_{ta}, and masses, M, of structures at an epoch $a = 0.50$ ($z = 1.00$), where the difference of the predicted values of I for different models is maximum, with fractional uncertainties:

$$f_R \equiv \frac{\sigma_R}{R_{\mathrm{ta}}(a)} \sim 0.05, \quad f_M \equiv \frac{\sigma_M}{M} \sim 0.3, \tag{5.1.3}$$

with σ_R and σ_M the uncertainties in radius and mass, respectively; i.e., supposing that we will be able to achieve at that epoch similar uncertainties, as those achieved for the local universe using current measurement techniques.

As an example of the sensitivity of our method in determining the value of the cosmological constant, we consider the following question: how many structures we have to examine in order to establish with confidence that $\Lambda \neq 0$? Here we work in a model with $\Omega_{\mathrm{m},0} = 0.30$. In applying this method, trying to prove locally the existence of Λ, we can use results of other methods of getting the matter density of the Universe (BAO's, galaxy clusters) since they are also –in the sense described in the previous sub-section– local methods and do not harm the locality

of the test. Of course, measuring the matter density of the Universe using our method is also possible, since the difference in matter density affects the evolution of $I(a)$, but this would make much more complicated the practical implementation of the test.

In what follows, we consider that a (through z) can be measured with much higher accuracy than masses and radii of structures, so it is not a source of error in our calculations and it is treated just as a parameter. By measuring the turnaround radius and the mass of a structure, a value of $I(a)$ can be obtained (by rearranging eq. (4.3.10)):

$$I(a) = \log\left(\frac{R_{\rm ta}(a)}{R^*}\right) - \frac{1}{3}\log\left(\frac{M}{M^*}\right). \tag{5.1.4}$$

Errors in the measurements of radius and mass result in an uncertainty, σ_I, in the calculated value of I. Error propagation gives [19]:

$$\sigma_I^2 = \frac{1}{\ln^2 10}\left(\frac{1}{9}\frac{\sigma_M^2}{M^2} + \frac{\sigma_R^2}{R_{\rm ta}^2(a)}\right) \Rightarrow \sigma_I = \frac{1}{\ln 10}\left(\frac{1}{9}f_M^2 + f_R^2\right)^{1/2}, \tag{5.1.5}$$

where we have used the definitions of f_M and f_R. Plugging the values for f_M and f_R presented in eq. (5.1.3), we get:

$$\sigma_I \sim 0.05. \tag{5.1.6}$$

Let us now imagine that we perform N measurements of masses and radii of N different structures (for simplicity, consider that we measure all N structure exactly at $a = 0.50$) and we get N different values for I. Denote this mean value $\langle I\rangle$. If all values have the same error σ_I, (all measurements have the same fractional errors f_R and f_M), then the error of the mean, $\sigma_{\langle I\rangle}$, will be

$$\sigma_{\langle I\rangle} = \frac{\sigma_I}{\sqrt{N}}. \tag{5.1.7}$$

From the above equation we can find the number of measurements we have to perform in order to get a particular error in the mean $\langle I\rangle$, $\sigma_{\langle I\rangle}$, assuming that the error of every individual value of I is the same and equal to σ_I:

$$N = \left(\frac{\sigma_I}{\sigma_{\langle I\rangle}}\right)^2 \tag{5.1.8}$$

Figure 5.3 presents the inferred value for $\Omega_{\Lambda,0}$ for any measured value of I at an epoch $a = 0.50$. Suppose now that we measure a mean value of I about -0.400 which corresponds to a value for $\Omega_{\Lambda,0} \sim 0.68$, the value inferred from other techniques. To establish a 5σ confidence that $\Omega_{\Lambda,0} \neq 0$, we demand this observed mean value of I to be five standard deviations away from the value of I which corresponds to zero value for the cosmological constant, which is $I \sim -0.450$ (from fig. 5.3). This allows us to calculate the value of the error in the mean that establishes the desired confidence:

$$5\sigma_{\langle I\rangle} = -0.400 - (-0.450) \Rightarrow \sigma_{\langle I\rangle} \sim 0.01 \tag{5.1.9}$$

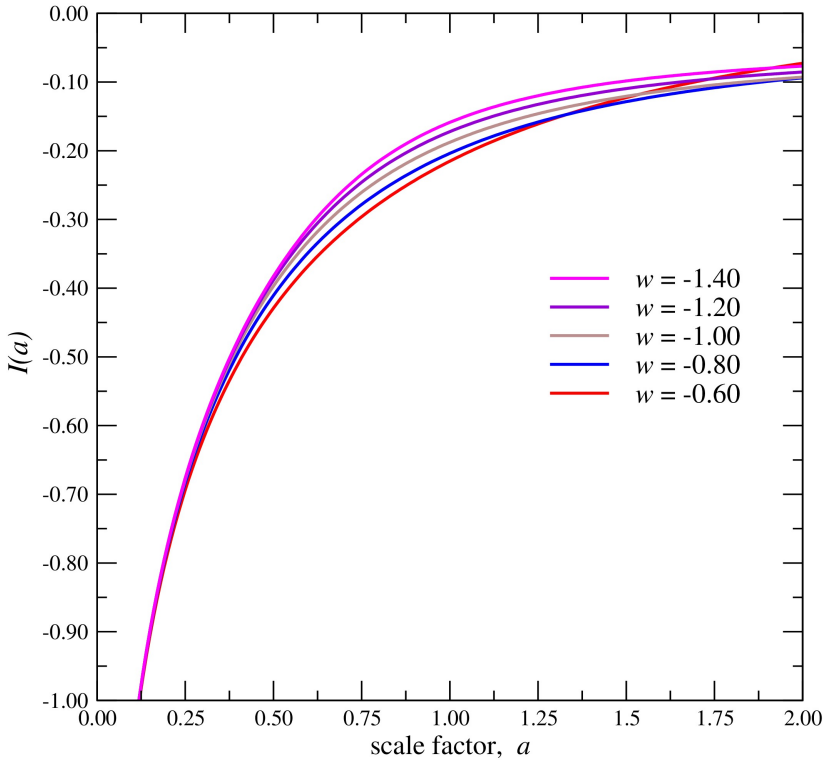

Figure 5.4: The evolution of $I(a)$ as a function of a, for constant dark energy density $\Omega_{\mathrm{de},0} = 0$ and matter density $\Omega_{\mathrm{m},0} = 0.30$, but different values of the equation of state parameter w. The case presented in this figure is models of clustering dark energy.

If all measurements of I have the same error, and equal to that presented in (5.1.6), then we can determine the number of measurements, N, we have to make to get the necessary accuracy in $\langle I \rangle$, from (5.1.8) :

$$N \sim \left(\frac{0.05}{0.01}\right)^2 = 25 \tag{5.1.10}$$

The above discussion, even with the simplifying assumptions that all structures are exactly at $a = 0.50$ and have the same uncertainties in mass and radius for all structures (also, extrapolating the current measurement techniques for the local universe to the universe at $a \sim 0.50$), gives a rough – order-of-magnitude – estimation of the number of measurements that have to be done in order to confidently establish a local proof that a non-zero cosmological constant exists.

5.2 Clustering Dark Energy

In figure 5.4, the evolution of the turnaround radius (through the parameter I) is presented for different values of w and constant $\Omega_{\mathrm{de},0} = 0$ and $\Omega_{\mathrm{m},0} = 0.30$. The results presented here correspond to clustering dark energy, such that presented in section 4.4.3. We see that, as expected, models with greater (less negative) w affect less significantly the evolution of the turnaround radius. We also see that different models present different values for I today.

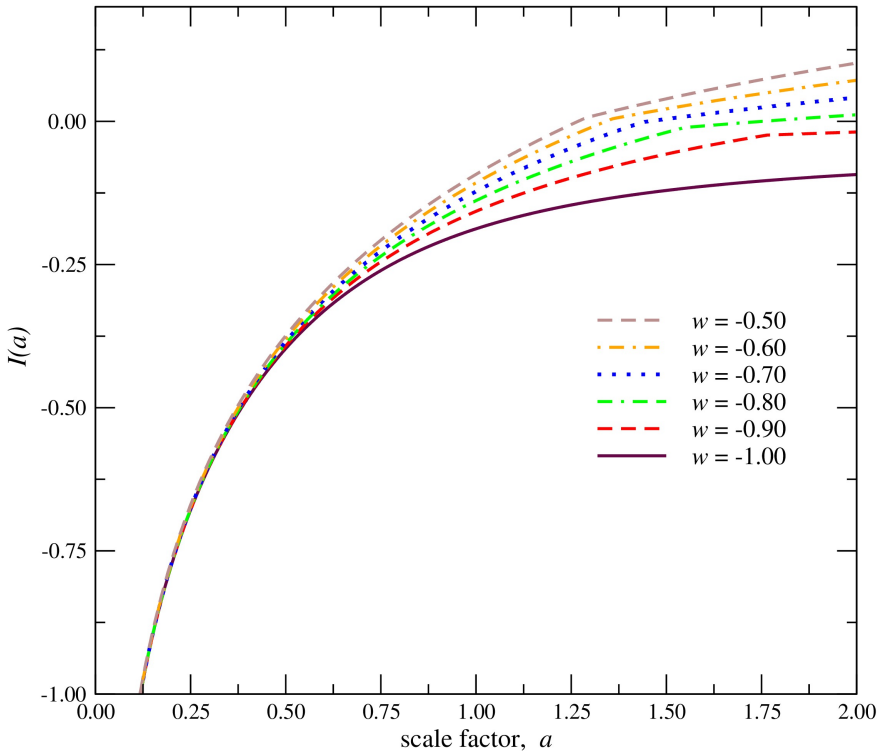

Figure 5.5: The evolution of $I(a)$ over cosmic time, a, for homogeneous dark energy models with different equation of state parameters ($w \geq 1$, quintessence). The values of dark energy density and matter density parameters are considered constant and equal to $\Omega_{\mathrm{de},0} = 0$ and $\Omega_{\mathrm{m},0} = 0.30$.

5.3 Homogeneous Dark Energy

We now turn to **homogeneous** dark energy, as described in section 4.4.4. Homogeneous dark energy with a more general equation of state parameter is widely considered as the best viable alternative to a cosmological constant, although current observations point out to an eq. of state parameter very close to -1.

5.3.1 Quintessence

In figure 5.5 we present the evolution of the parameter $I(a)$ for quintessence models ($w \geq -1$), with all models having constant dark energy density $\Omega_{\mathrm{de},0} = 0$ and matter density $\Omega_{\mathrm{m},0} = 0.30$. In the figure we see that the curves smoothly approach that which corresponds to $w = -1$ (cosmological constant) which has independently calculated previously.

An important feature is that models with different w have different values of I today. In figure 5.7, we present the value of I today as a function of the equation of state parameter w. This shows that it is in principle possible to use measurements of turnaround radii in the present epoch to probe dark energy and its eq. of state parameter.

Also as expected for two models 1 and 2, with $w_1 > w_2$ (less negative) we always have $I_1 > I_2$. Models with higher w produce a less stronger antigravitational effect on cosmic structure and thus the formation of structure becomes easier. Thus, a smaller value of the overdensity δ is required for turnaround. From the functional form of $I(a)$, eq. (4.3.9), we thus understand that I must be higher for such a

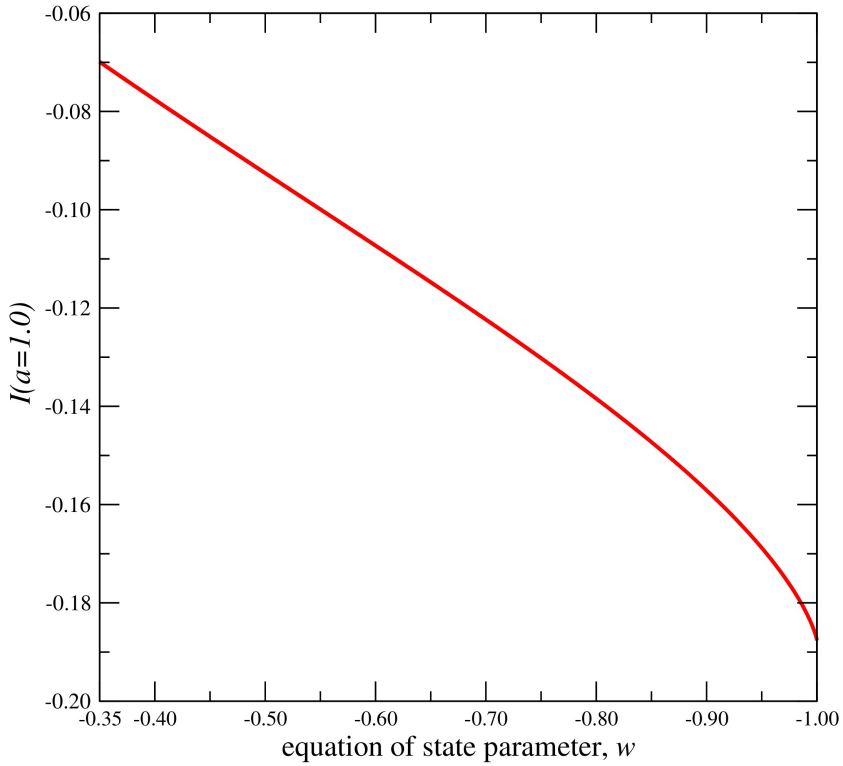

Figure 5.6: The value of I today, as a function of the value of the equation of state parameter w ($w \geq 1$, quintessence). All models have $\Omega_{\mathrm{de},0} = 0$ and $\Omega_{\mathrm{m},0} = 0.30$.

model. For $w > -1$ the maximum turnaround radius $\to \infty$.

5.3.2 Phantom Energy

In figure 5.7, we present the evolution of I for a dark energy equation of state < -1 (phantom energy). Again, the models have different value of w but they have constant dark energy density $\Omega_{\mathrm{de},0} = 0$ and matter density $\Omega_{\mathrm{m},0} = 0.30$. Here we can see qualitative differences with the case of quintessence.

First of all, all models have the same value for I today. This is different than the previous case, where we all models had the same value in the distant past and different values today. Secondly, for two models with $w_1 > w_2$, we have: for $a < 1$ (in the past)$I_2 > I_1$, while for $w_2 > w_1$ (in the future) we have $I_1 > I_2$. Third, the models do not approach smoothly the curve with $w = -1$ cosmological constant. We have not explained yet this issue and thus we present our results only as preliminary results that need further investigation and study.

The behaviour of the curves that seems to be correct is that the value of I decreases as a function of a for all models. Phantom energy has a super-negative equation of state parameter, and it is a stronger anti-gravity than the cosmological constant. As the time passes, the dark energy density increases and becomes more and more dominant. Thus a higher overdensity is required for turnaround. From the functional form of I, we then can see why I should decrease with time in phantom energy models.

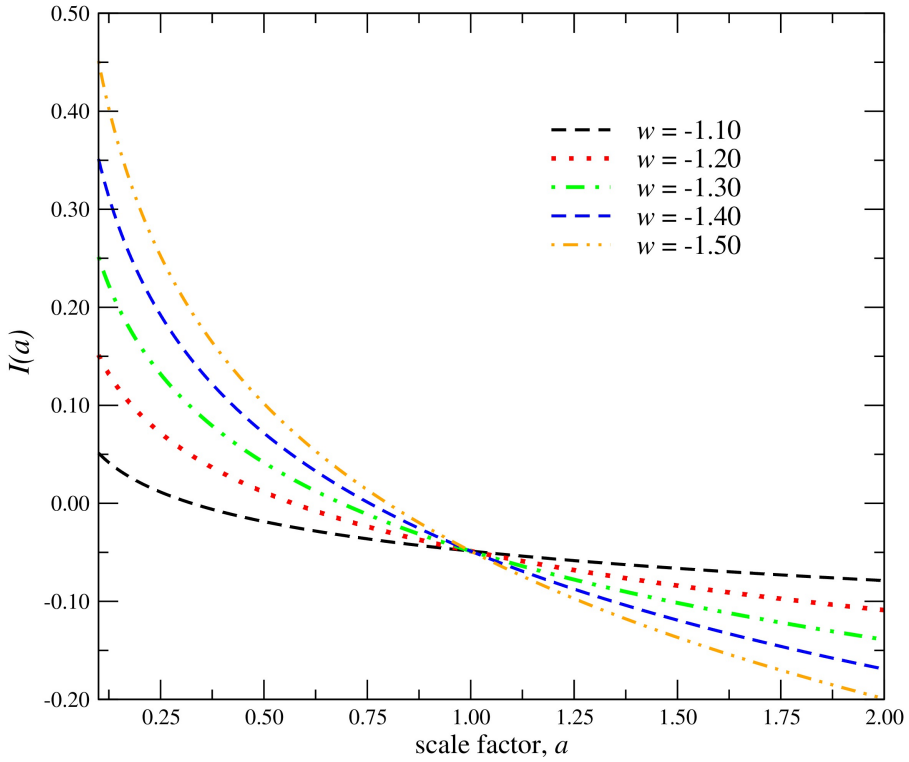

Figure 5.7: The evolution of $I(a)$ over cosmic time, a, for homogeneous dark energy models with different equation of state parameters ($w \leq 1$, phantom energy). The values of dark energy density and matter density parameters are considered constant and equal to $\Omega_{\mathrm{de},0} = 0$ and $\Omega_{\mathrm{m},0} = 0.30$.

Chapter 6

Outlook

Based on the need for the cosmological constant to be weak enough to allow gravitational bound structures to form, anthropic arguments have long before used to set upper bounds for its value, see for example the seminal paper of Weinberg (1987). Detailed studies concerning galaxy formation put tighter upper bounds for the value of $\Omega_{\Lambda,0}$, turned out to be very close to the value inferred later from the measured accelerated expansion of the Universe.

In the present work, we used structure formation to demonstrate a way not only to set a local upper bound for the cosmological constant but rather to show that a local **measurement** of $\Omega_{\Lambda,0}$ is in principle possible. Especially that it is easy to use the evolution of the turnaround radius of cosmic structures in order to set a **lower** bound to the value of $\Omega_{\Lambda,0}$ – in other words, to obtain a local proof that the cosmological constant has a non-vanishing value. The merits of such a proof (or disproof) have been discussed in the introduction.

In our work we have mainly been focused on how to use the evolution of the turnaround radius to measure the cosmological constant, not the matter density of the Universe. However, measuring the matter density using this method it is also possible, in principle. We have seen that today the value of the turnaround radius (or the function $I(a)$ defined in the text, today) has a extremely weak dependence on $\Omega_{\Lambda,0}$ but depends on the value of $\Omega_{\mathrm{m},0}$. Thus, using observations from the very close Universe we can determine the value of the matter density and then use it as an input, in order to measure the cosmological constant by going backwards in time, i.e. to the distant Universe. Although it is important that this method can be used to measure both parameters, in practice this would be quite complex. If our target is a local measurement of the cosmological constant, we can use as input for the value of matter density of the Universe the value obtained using other methods, which are also local.

A similar analysis has been given for the case of a dark energy with a more general equation of state parameter, w, for the clustering and homogeneous case. A obvious extension would be to consider a general, time dependent equation of state parameter, $w(a)$. Solving the spherical collapse model in modified gravity models and thus obtaining the time evolution of the turnaround radius seems in principle possible. However none of these is presented here; we hope to address these issues in future work.

Our analysis is based on the spherical collapse model, which is a simple model

for the description of structure formation. However, we expect the results presented here to hold at least qualitatively. Indeed, the effect of non-sphericities is not expected to be severe at turnaround scales. Since our aim was to give a proof-of-principle about the ability to use the evolution of the turnaround radius in order to measure cosmological parameters –especially the value of the cosmological constant and the equation of state parameter– the treatment presented here is adequate. The implementation of this idea is not easy, and before using actual observations, in order to get accurate values for $\Omega_{\mathrm{m},0}$, $\Omega_{\Lambda,0}$, and w the evolution of I has to be benchmarked at higher accuracy using numerical simulations.

Bibliography

[1] Addison, G. E., Hinshaw, G., & Halpern, M. 2013, MNRAS, 436, 1674

[2] Amendola, L., Appleby, S., Bacon, D., et al. 2013, Living Reviews in Relativity, 16,

[3] Amendola, L., & Tsujikawa, S. 2010, Dark Energy : Theory and Observations by Luca Amendola and Shinji Tsujikawa. Cambridge University Press, 2010. ISBN: 9780521516006,

[4] Barrow, J. D., & Saich, P. 1993, MNRAS, 262,

[5] Busha, M. T., Adams, F. C., Wechsler, R. H., & Evrard, A. E. 2003, ApJ, 596, 713

[6] Busha, M. T., Evrard, A. E., Adams, F. C., & Wechsler, R. H. 2005, MNRAS, 363, L11

[7] Cai, Y.-F., Saridakis, E. N., Setare, M. R., & Xia, J.-Q. 2010, PhysRep, 493, 1

[8] Caldwell, R. R. 2002, Physics Letters B, 545, 23

[9] Carroll, S. M. 2001, Living Reviews in Relativity, 4,

[10] Carroll, S. M., Hoffman, M., & Trodden, M. 2003, PhysRevD, 68, 023509

[11] Clifton, T., Ferreira, P. G., Padilla, A., & Skordis, C. 2012, PhysRep, 513, 1

[12] Dolgov, A. D., & Kawasaki, M. 2003, Physics Letters B, 573, 1

[13] Durrer, R., & Straumann, N. 1990, MNRAS, 242, 221

[14] Eisenstein, D. J., Zehavi, I., Hogg, D. W., et al. 2005, ApJ, 633, 560

[15] Eke, V. R., Cole, S., & Frenk, C. S. 1996, MNRAS, 282, 263

[16] Enqvist, K. 2008, General Relativity and Gravitation, 40, 451

[17] Frieman, J. A., Turner, M. S., & Huterer, D. 2008, ARA& A, 46, 385

[18] Garcia-Bellido, J., & Haugbølle, T. 2008, JCAP, 4, 003

[19] Hughes, Ifan and Hase, Thomas P. A. (2010) Measurements and their uncertainties : a practical guide to modern error analysis. Oxford : New York, NY: Oxford University Press. ISBN 9780199566327

[20] Iribarrem, A., Andreani, P., February, S., et al. 2014, A& A, 563, A20

[21] Joyce, A., Jain, B., Khoury, J., & Trodden, M. 2015, PhysRep, 568, 1

[22] Khoury, J. 2010, arXiv:1011.5909

[23] Lokas, E. L., & Hoffman, Y. 2001, Identification of Dark Matter, 121

[24] Mortonson, M. J., Weinberg, D. H., & White, M. 2013, arXiv:1401.0046

[25] Padmanabhan, T. 1995, Structure formation in the universe (Cambridge University Press)

[26] Pavlidou, V., & Fields, B. D. 2005, PhysRevD, 71, 043510

[27] Pavlidou, V., & Tomaras, T. N. 2014, JCAP, 9, 020

[28] Peebles, P. J. E. 1980, Research supported by the National Science Foundation. Princeton, N.J., Princeton University Press, 1980. 435 p.,

[29] Peebles, P. J., & Ratra, B. 2003, Reviews of Modern Physics, 75, 559

[30] Percival, W. J. 2005, A& A, 443, 819

[31] Perlmutter, S., Aldering, G., Goldhaber, G., et al. 1999, ApJ, 517, 565

[32] Planck Collaboration, Ade, P. A. R., Aghanim, N., et al. 2015, arXiv:1502.01589

[33] Planck Collaboration, Ade, P. A. R., Aghanim, N., et al. 2015, arXiv:1502.01590

[34] Riess, A. G., Filippenko, A. V., Challis, P., et al. 1998, AJ, 116, 1009

[35] Samushia, L., Reid, B. A., White, M., et al. 2013, MNRAS, 429, 1514

[36] Schmidt, B. P., Suntzeff, N. B., Phillips, M. M., et al. 1998, ApJ, 507, 46

[37] Sundell, P., Mörtsell, E., & Vilja, I. 2015, JCAP, 8, 037

[38] Tanoglidis, D., Pavlidou, V., & Tomaras, T. N. 2015, JCAP, 12, 060

[39] Tanoglidis, D., Pavlidou, V., & Tomaras, T. 2016, arXiv:1601.03740

[40] Weinberg, D. H., Mortonson, M. J., Eisenstein, D. J., et al. 2013, PhysRep, 530, 87

[41] Weinberg, S. 1987, Physical Review Letters, 59, 2607